Journal of Hazardous Materials 211–212 (2012) 30–46

Contents lists available at SciVerse ScienceDirect

Journal of Hazardous Materials

journal homepage: www.elsevier.com/locate/jhazmat

Review

# Bi-component semiconductor oxide photoanodes for the photoelectrocatalytic oxidation of organic solutes and vapours: A short review with emphasis to $TiO_2$–$WO_3$ photoanodes

J. Georgieva[b], E. Valova[b], S. Armyanov[b], N. Philippidis[a], I. Poulios[a], S. Sotiropoulos[a,*]

[a] Department of Chemistry, Aristotle University of Thessaloniki, Thessaloniki 54124, Greece
[b] Rostislaw Kaischew Institute of Physical Chemistry, Bulgarian Academy of Sciences, Sofia 1113, Bulgaria

ARTICLE INFO

*Article history:*
Received 22 October 2011
Received in revised form
19 November 2011
Accepted 21 November 2011
Available online 28 November 2011

*Keywords:*
Photocatalysis
Semiconductor oxide
Photo-oxidation
$TiO_2$
$WO_3$

ABSTRACT

The use of binary semiconductor oxide anodes for the photoelectrocatalytic oxidation of organic species (both in solution and gas phase) is reviewed. In the first part of the review, the principle of electrically assisted photocatalysis is presented, the preparation methods for the most common semiconductor oxide catalysts are briefly mentioned, while the advantages of appropriately chosen semiconductor combinations for efficient UV and visible (vis) light utilization are highlighted. The second part of the review focuses on the discussion of $TiO_2$–$WO_3$ photoanodes (among the most studied bi-component semiconductor oxide systems) and in particular on coatings prepared by electrodeposition/electrosynthesis or powder mixtures (the focus of the authors' research during recent years). Studies concerning the microscopic, spectroscopic and photoelectrochemical characterization of the catalysts are presented and examples of photoanode activity towards typical dissolved organic contaminants as well as organic vapours are given. Particular emphasis is paid to: (*a*) The dependence of photoactivity on catalyst morphology and composition and (*b*) the possibility of carrying out photoelectrochemistry in all-solid cells, thus opening up the opportunity for photoelectrocatalytic air treatment.



**Contents**



* Corresponding author. Tel.: +30 2310 997742; fax: +30 2310 443922.
*E-mail addresses:* eczss@otenet.gr, eczss@chem.auth.gr (S. Sotiropoulos).

0304-3894/$ – see front matter © 2011 Elsevier B.V. All rights reserved.
doi:10.1016/j.jhazmat.2011.11.069

## 1. Photoelectrocatalytic oxidation of organics at semiconductor anodes: principle and advantages

A promising advanced oxidation technology for effluent treatment and decontamination of water and air (that can result in principle in complete mineralization of organic pollutants or contaminants) is that of heterogeneous photocatalysis [1–3]. When a semiconductor catalyst is illuminated by ultraviolet (UV) or visible (vis) light the photogenerated holes at the valence band react with water and produce $OH^{\bullet}$ radicals while the photogenerated electrons at the conduction band react with oxygen and produce superoxide radicals. Both of these primary products (in particular $OH^{\bullet}$ radicals) have a high oxidizing power and attack organic pollutants and microorganisms. Some organic species can also undergo direct photooxidation by direct scavenging of holes. The process has a number of advantages: (*i*) The catalysts used are inexpensive, environmentally friendly and recyclable; (*ii*) the exciting radiation is UV light (310–380 nm, UVA) of low power requirements (1–5 W $m^{-2}$ of catalyst surface area), while even visible light radiation is to a smaller extent effective. This means that solar radiation can be used in many cases; (*iii*) the only oxidant needed is molecular oxygen and the process is carried out at room temperature and under atmospheric pressure.

The catalyst (usually a semiconductor oxide and, in most practical cases, titanium dioxide) is used either as a slurry suspension (as an air-suspension in the case of air treatment) or supported on solid substrates. In the former case the powder photocatalyst is suspended as fine particles and mass transfer limitations are minimized. Also, the high surface-to-volume ratio in that case ensures high light utilization efficiency (since only holes generated close to the surface manage to diffuse to the surface and to be used as oxidants before recombination with electrons occurs). At the same time however, the use of fine particles entails very long sedimentation times or fine filters for the catalyst to be removed from the purified medium. Hence, the use of supported photocatalysts instead of catalyst slurries or suspensions offers some advantages namely, the absence of the costly step of catalyst separation as well as a modular design of the treatment cell [5–7]. The small total surface area and mass transport limitations constitute, on the other hand, drawbacks of supported catalysts.

An approach to offset some of the disadvantages of supported semiconductor photocatalysts is their immobilization on an electronic conductor and the application of an external voltage (of the order of a few volts) in an appropriate electrochemical cell, where the semiconductor catalyst is a part of the (photo) anode while a metal or carbon is the electronic conductor used as a cathode, as depicted in Fig. 1. In this arrangement the photogenerated electrons are drawn away from the catalyst surface via the external circuit while photogenerated holes are transferred to the electrode surface. Therefore the rate of electron–hole recombination is limited and the rate of surface reactions increased. This enhanced photocatalytic process is known as photoelectrocatalysis (PEC) or electrically enhanced photocatalysis [8–24].

Since in PEC photogenerated electrons need not be scavenged by $O_2$ (as they are drawn by the positive bias) and the applied voltage is usually sufficient to drive water reduction at the cathode of the cell (instead of oxygen reduction), there is usually no need for constant oxygen levels in the medium and, consequently, no need for continuous air purging. At the same time, the reactions occurring at the cathode offer additional opportunities: water electrolysis can lead to simultaneous $H_2$ production [25] while harmful metal ions can be deposited as pure metal and removed from the effluent [26]. Water electrolysis/$H_2$ production can be the sole process taking place at the cathode if there are no other reducible species in excess (such as metal ions or continuously purged oxygen) and a good hydrogen evolution cathode is chosen (e.g. Pt, Ni or stainless steel). The presence of a photo-anode leads to a significant lowering of the applied voltage needed for water electrolysis; higher hydrogen production rates at lower applied biases can be attained in practice if an excess of photo-oxidized species (e.g. dyes or sugars) are present in the photoanode compartment (simultaneous organics detoxification and hydrogen production [25]).

One of the first papers that proposed PEC for decontamination applications (sterilization of microbial cells) appeared in the mid 80s and was due to Matsunaga et al. [8]. It was not until the mid 90s however that the method started to establish among electrochemists as a viable means of organics destruction, as indicated by papers of Anderson and co-worker [9], Augustynski and co-workers [10], Enea [11] and Christensen and co-workers [12,13]. That work was shortly followed by applied research papers by Byrne and Eggins [14] and Fernandez-Ibanez et al. [15]. During the last decade, many more publications appeared on the subject of photoelectrocatalytic water treatment (see for example [16–24] and in particular the review of [20]).

There have been however much fewer papers on photoelectrocatalytic air treatment. The first report on alcohol vapour

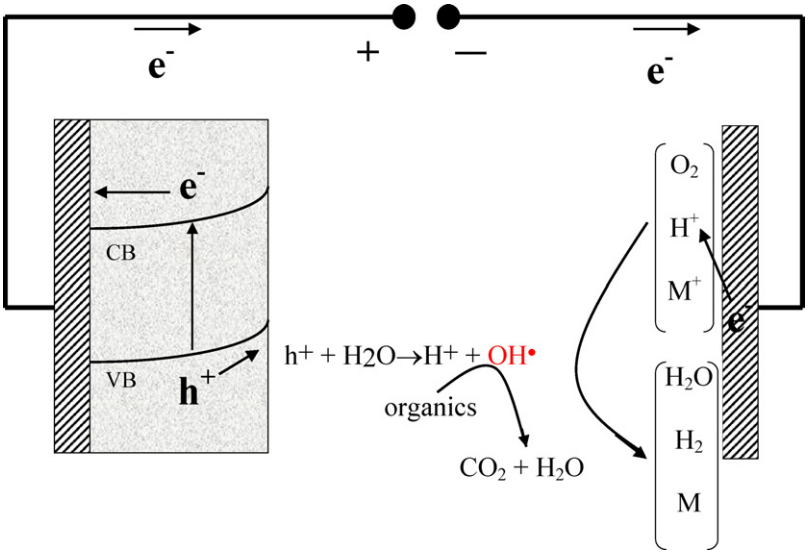


**Fig. 1.** Schematic representation of a photoelectrocatalytic cell for the electrochemically assisted photooxidation of organics.

photoelectrochemical oxidation was due to Enea [11] who used the $TiO_2$-coated porous glass wall of a liquid electrolyte cell as the photoanode. The first all-solid device for gas photo-electro-oxidation was of a photodiode type whereby $TiO_2$ was sandwiched between ITO electrodes and a high voltage (tens of volts) was applied [27]. Although most of dye-sensitized solar cells employ a solid polymer or gel electrolyte (see for example [28,29]), there have been very few reports until recently on polymer-supported $TiO_2$ photoanodes [30–32] as a part of a solid polymer electrolyte cell. These were devoted to $CO_2$ reduction [30,31] or hydrogen production [32] at the cathode. All-solid Nafion®-based photoelectrochemical cells for organic vapour photooxidation at $TiO_2/WO_3$ electrosynthesized coatings on a stainless steel mesh [33], at $TiO_2$ powders [34] or $TiO_2 + WO_3 + C$ [35] powder mixtures, have only recently been introduced and could be the basis of practical devices for air-treatment (schematic representations of such devices are given later).

## 2. Semiconductor oxide photocatalysts: overview and preparation methods

### 2.1. Overview of common semiconductor oxide photocatalysts

The most popular photocatalyst is crystalline $TiO_2$, a wide gap n-type semiconductor activated by UV light [4] from solar or artificial radiation sources and used either in a slurry or supported layer form. $TiO_2$ is reported as the most promising material because of its high efficiency and low cost [36]. Other advantages include the fact that it is a safe, chemically and photochemically resistant material and that both itself and its doped variants can be prepared by a variety of methods (e.g. sol–gel, hydrothermal, etc. – see also below). The anatase crystallographic form of $TiO_2$ (with an energy band gap of $E_g = 3.2$ eV) is generally accepted as more photoactive than the rutile one (with $E_g = 3.0$ eV) due to a difference in electronic, chemical and adsorption properties [37], but mixtures of the two are often found to be optimum. This is also the case of the commercially available Degussa P-25® $TiO_2$ photocatalyst (70% anatase, 30% rutile) which is universally accepted as the best formulation in most photocatalysis applications [38–40].

$WO_3$ is rarely used alone but is a promising additive for $TiO_2$ since it modifies its photochemical properties in a favourable manner both with respect to reduced recombination and visible light activity (see below). Due to a variety of possible types of light excitation [41], $WO_3$ has a broad range of band-gap values ($E_g = 2.6$–$3.3$ eV) that have been reported in the literature [41–44]; the fundamental optical transition is of an indirect type with $E_g = 2.7$–$2.8$ eV [42,45], thus ensuring considerable photocatalytic and photoelectrocatalytic activity for $WO_3$ even under visible light illumination [46–48].

ZnO is the commonest alternative to $TiO_2$ in semiconductor photocatalysis [49–51], with a similar energy band gap ($E_g = 3.3$ eV) [52,53], low-cost and non-toxicity. It can be prepared in a variety of forms and structures and it has comparable photocatalytic activity to $TiO_2$, but is known to photo-corrode.

$Cu_2O$ (and CuO) is a p-type semiconductor with a band-gap energy of 1.8–2.5 eV (and 1.21–2.00 eV, respectively) [54–57] that absorbs visible light and is abundant. (Note that $Cu_2O$ can also be prepared as an n-type semiconductor, although with much more difficulty.) Although it is mainly used in solar cells, applications in organics photo-oxidation have also appeared in the literature [58–60].

$Fe_2O_3$ (in its $\alpha$-$Fe_2O_3$, hematite form) is another example of visible light active semiconductor oxide ($E_g \approx 2.2$ eV) [61,62] that, although it does not photocorrode and has reasonable chemical stability, the location of its valence and conduction bands do not favour OH radical or hydrogen production, respectively, hence making it an ineffective photocatalyst for organics oxidation or hydrogen production, respectively, when used on its own [63]. Its coupling with other semiconductors and/or the application of a appropriate bias [64] is therefore necessary.

Another semiconductor oxide that has recently drawn attention to is $Bi_2O_3$ which can be either of a p- or n-type [65]. Its bad-gap being 2.8 eV, it exhibits visible light activity too and it is mainly used in combination with other semiconductors [66–69].

Finally, there are also many single phase mixed oxides with semiconducting properties of which strontium titanate, $SrTiO_3$ (see for example [70–72]) and bismuth vanadate, $BiVO_4$, (see for example [68,73,74] are the most characteristic examples. $SrTiO_3$ has the same energy band gap as $TiO_2$ (3.2 eV [75]) and (similar to $TiO_2$ and ZnO) can be used alone as an efficient photocatalyst for organics electrooxidation since its valence and conduction bands are at energy levels able to produce OH radicals from water oxidation and superoxide radicals by oxygen reduction [76]. On the other hand, $BiVO_4$ (with a band gap of 2.8 eV [68]) is mainly used as a visible-active additive to other semiconductors [68,73,74].

### 2.2. Preparation methods of common semiconductor oxides

#### 2.2.1. Non-electrochemical methods

In this section, we briefly mention the most common non-electrochemical methods for the preparation of semiconductor oxides and the corresponding photoanode coatings.

The most widespread method of semiconductor powder formation is the sol–gel preparation route and its variants, realized either by hydrolysis, chemical precipitation or solvothermal methods. $TiO_2$ nanoparticle powders are usually obtained by the sol–gel method from hydrolysis of a titanium precursor (see for example Refs. [77–81]); this often entails the acid-catalyzed hydrolysis of titanium(IV) alkoxide and subsequent condensation (see for example [82–85]). Hydrothermal preparation of $TiO_2$ under controlled temperature and/or pressure with the reaction in aqueous solutions is an alternative route [86–89]. $WO_3$ powders can also be produced by sol–gel/chemical precipitation methods (see for example [90]) and so are ZnO [91,92], $Fe_2O_3$ [93–95], $SnO_2$ [96–98], $Bi_2O_3$ [99,100] and $Cu_2O$ [101].

Typically, suspensions of the thus produced oxide nanoparticles (either commercially available or prepared in the laboratory) are used for film preparation by dip-coating, spraying or sedimentation techniques [102–104]. For the production of uniform coatings with controlled porosity, polyethylene glycol (PEG) is often added to the suspension and subsequently burnt off during annealing at temperatures higher than 400–500 °C (see for example [105,106]).

Semiconductor films can be prepared directly onto various substrates (including electrode substrates) by sputtering/pulsed-layer-deposition/magnetic sputtering (see [93,107,108] for $Fe_2O_3$ and $Cu_2O$), spray pyrolysis techniques ([109–116] for $TiO_2$ and $WO_3$, [117,118] for $Fe_2O_3$, [119] for ZnO) or chemical vapour deposition (CVD) ([120–126] for $TiO_2$ and $WO_3$, [127,128] for $Fe_2O_3$ and [129] for ZnO).

Finally, all semiconductor oxide films can be simply prepared by thermal treatment of the corresponding metals whereby the oxide is formed and grows at the annealing temperature (see for example [130–132] for $TiO_2$ and $WO_3$, [133] for $Bi_2O_3$ and [134] for $Fe_2O_3$).

#### 2.2.2. Electrochemical methods

Electrochemical methods have been proposed as alternative methods for the production of semiconductor layers on conducting substrates, to be used either in solar cell or organics photooxidation applications, since they offer a number of advantages namely, simplicity of equipment, accurate control of layer thickness and applicability to substrates of complex shapes. Following their

electrochemical preparation, all oxides are annealed at an appropriate temperature to obtain the desired crystalline structure for semiconductor behaviour.

*2.2.2.1. Cathodic electrosynthesis and electrodeposition.*

*2.2.2.1.1. Cathodic electrosynthesis of $TiO_2$, ZnO and $Fe_2O_3$ coatings.* The principle of the technique lies on the deposition of the corresponding metal oxide or hydroxide on the electrode surface due to local solution alkalization during the operation of the substrate as a cathode in an electrolytic cell.

The main approach for $TiO_2$ cathodic electrosynthesis is that of DC controlled potential deposition on a variety of cathodes, as pioneered independently and almost simultaneously by Nogami and co-worker [135] and Zhitomirski and co-workers [136]. Both methods are based on the precipitation of titanium hydroxide or oxohydroxide from the reaction of stabilized Ti(IV) species with hydroxyl ions, produced as a result of alkalization during nitrate reduction at the cathode substrate:

$$NO_3^- + H_2O + 2e^- \rightarrow NO_2^- + 2OH^- \quad (1)$$

In the former method, as adopted by Rajeshwar and co-workers [137,138] or modified by Minoura and co-workers [139,140] as well as our groups (see references in the next section), titanyl ions (produced by dissolution of Ti metal [137,138]) or peroxotitanium complexes (produced by stabilization of $TiOSO_4$ with $H_2O_2$ [139,140]) react in aqueous solutions with $OH^-$ to give:

$$TiO^{2+} + 2OH^- + xH_2O \rightarrow TiO(OH)_2{\cdot}xH_2O \quad (2)$$

or

$$TiOSO_4 + H_2O_2 \rightarrow Ti(O_2)SO_4 + H_2O \quad (3)$$

$$Ti(O_2)SO_4 + 2OH^- + (x+1)H_2O \rightarrow TiO(OH)_2{\cdot}xH_2O + H_2O_2 + {SO_4}^{2-} \quad (4)$$

In the latter method, as further developed by Zhitomirski and co-workers [141–145] and (expanded to other oxides too), $TiCl_4$ was dissolved in an organic solvent and stabilized with aqueous $H_2O_2$ to form again a stable peroxo-complex that was further hydrolyzed by $OH^-$ produced at the cathode:

$$Ti^{4+} + H_2O_2 + (n-2)H_2O \rightarrow [Ti(O_2)(OH)_{n-2}]^{(4-n)+} + nH^+ \quad (5)$$

$$Ti(O_2)(OH)_{n-2}]^{(4-n)+} + mOH^- + kH_2O \rightarrow TiO_3(H_2O)_x. \quad (6)$$

Thermal decomposition of the hydrated products of (2), (4) or (6), results in crystalline $TiO_2$. Zhitomirsky and co-workers have deposited $TiO_2$ on Pt, graphite, carbon felts and Ti but the majority of other researchers (Nogumi, Minoura, Rajeshwar and co-workers), who tested the photocatalytic or electrochromic properties of the deposits, have employed optically transparent electrodes. Our groups have prepared and tested photoelectrodes of electrosynthesized $TiO_2$ on economical stainless steel substrates (see references in next section). It should be noted that the single report of electrosynthesized $TiO_2$ on stainless steel [146] (prior to the above-mentioned reports) dealt with deposition from an acetone-$J_2$ bath with a sacrificial Ti anode and that no microscopic or photoelectrochemical characterization of the material was presented therein.

An alternative approach for $TiO_2$ electrosynthesis, based again on Ti hydroxide precipitation due to solution alkalization at the cathode, is that of AC deposition onto hard alumite ($Al/Al_2O_3$), established by Ishikawa, Matsumoto and co-workers [147–150]. The aluminium substrate was etched by immersion in an alkaline solution and then electrochemically oxidized at 20 mA $cm^{-2}$ in $H_2SO_4$ solution to prepare the porous hard alumite on its surface. $TiO_2$ was electrodeposited by alternate current electrolysis with a bias of few tens of volts and a frequency of 60 Hz, from a mixed aqueous solution of $(NH_4)_2[TiO(C_2O_4)_2]$ and $(COOH)_2$ adjusted to pH 4. The amount of deposited $TiO_2$ did not depend on the ac voltage, and the deposition occurred even under no bias, with electrodeposition predominantly occurring in the region below 50 °C, while chemical deposition at temperatures higher than about 50 °C.

Finally, one should mention another two techniques for the preparation of $TiO_2$ photocatalytic coatings that, although they cannot be classified as electrosynthesis of $TiO_2$, they involve the application of an electric field. The first is the occlusion of $TiO_2$ particles during the electrodeposition of a metallic, conducting polymer or other semiconductor layer (see for example references [137,138,151–154]). The second is the electrophoretic deposition of $TiO_2$ from appropriate suspensions onto cathodically biased substrates (see for example [155]).

Cathodic electrodeposition is now one of the most popular approaches for ZnO growth in various nanostructured arrangements [156–162]. The deposition is carried out at high negative potentials from neutral solutions of $Zn(NO_3)_2$ or $ZnCl_2$, sometimes with the saturation of the solution with oxygen.

$Fe_2O_3$ can be formed cathodically too from Fe(III) solutions containing $H_2O_2$ which produces $OH^-$ upon its reduction at the cathode substrate (see for example [163,164]). $OH^-$ reacts with Fe(III) to form insoluble FeOOH which is transformed to the corresponding semiconductor oxide following annealing.

*2.2.2.1.2. Cathodic electrodeposition of $WO_3$ and $Cu_2O$ coatings.* $WO_3$ can be deposited on conducting substrates by direct electrodeposition that is realized via the cathodic reduction of the peroxotungstate species ${W_2O_{11}}^{-2}$ formed in tungstate solutions of acidic pH containing $H_2O_2$:

$${W_2O_{11}}^{2-} + 2H^+ + xe^- \rightarrow 2WO_3 + 2O_2 + H_2O. \quad (7)$$

There are many papers in the literature where tungsten trioxide films were prepared by cathodic electrodeposition and tested for their electrochromic or photoelectrochemical properties. The works of Hepel and co-workers [16,44,47], Rajeshwar, Pauporte, Tacconi and co-workers [165–167,137] as well as those of our groups [168–170] are typical of the use of cathodically produced $WO_3$ photoelectrodes in organics photooxidation (either as a single component coating or combined with $TiO_2$).

Cathodic electrodeposition of cuprous oxide ($Cu_2O$) is the commonest approach to produce this semiconductor oxide in controlled quantities and morphologies (see for example [57,158,171–173]). It is carried out from alkaline Cu(II) solutions at moderately negative potentials whereby Cu(II) is partially reduced to Cu(I) which, in the presence of $OH^-$, is deposited as $Cu_2O$.

*2.2.2.2. Anodization and anodic electrosynthesis.* $TiO_2$ microporous or ordered nanotubular coatings can be prepared from Ti substrates by galvanostatic or potentiostatic anodization in aggressive media such as mixtures of sulphuric, nitric and hydrofluoric acid, often with the addition of hydrogen peroxide too [174–179]. The applied voltage is usually in the few tens of volts range and the anodization period in the range of few hours. $WO_3$ photoelectrodes have also been prepared by anodic oxidation of W metal either at relatively low applied potential values [180,181] or at a few tens of volts [182,183]. The formation of $Cu_2O$ by a Cu foil anodization has also been reported [184].

Alternatively, $TiO_2$ can be electrosynthesized by the oxidation of Ti(III) on optically transparent electrodes or Pt substrates from slightly acidic $TiCl_3$ aqueous solutions by excursion of the electrode substrate potential to values of a few hundred millivolts (see for example [44,185]). In a similar manner, the oxidation of Fe(II) ions from neutral solutions (stabilized by ligands) or

slightly acidic solutions, leads to the formation of Fe(III) which is then precipitated as FeOOH (and transformed to $Fe_2O_3$ upon annealing) [64].

### 2.3. Photoanode substrates

In electrically enhanced photocatalysis the conducting substrates onto which the semiconductor catalysts are supported have usually been either optically transparent electrodes (OTEs) (see for example [137,167,186–188]) or Ti and its alloys (see for example [13,15,18,19]). Pt has also been used as a photoanode support [16,137] while more recently carbon [189] or carbon nanotubes (CNTs) [190,191] and boron-doped diamond (BDD) [192,193] have all served as photocatalytic electrode supports.

Despite the fact that stainless steel is a cheap and practical alternative substrate that has frequently been used in supported photocatalyst studies (see for example [194,195]) it has only recently been tested as an electrode substrate in photoelectrocatalysis, either for the photooxidation of organics [21,33,168–170] (in our laboratories) or in solar cells [196–198]. There are at least two problems that can be foreseen in the use of stainless steel supports for such applications. First, the possibility of stainless steel pitting corrosion or passivation breakdown from solution-exposed substrate areas at open circuit or under the positive bias used in photoelectrocatalysis. Second, the formation of stainless steel oxides between the substrate and the semiconductor upon thermal annealing and/or under a positive bias, may be detrimental for the effective application of the electric field. The former makes the need for uniform $TiO_2$ or/and $WO_3$ coatings paramount since such films are known to offer cathodic protection to stainless steel upon UV illumination by pumping of photogenerated electrons to the steel substrate; to that direction, PEG-containing $TiO_2$ films [21] or electrosynthesized $WO_3$ underlayers [168–170] offer a solution. The latter generally result in lower photocurrents–photoelectrochemical activity of $TiO_2$/SS electrodes when compared to $TiO_2$/Ti ones that could however be remedied by increasing the photocatalytic activity e.g. by dopants. Finally, the ability to produce large electrodes and to control the thickness of the semiconductor films and the quantity of the catalyst on an appropriate electrode support is of great importance since these parameters affect both the cost and the performance of the photoanode in practical applications.

## 3. Photocatalytic activity and synergism in bi-component semiconductor oxides

There are two main targets of research aiming at improving the efficiency of semiconductor oxides as photooxidation catalysts (usually $TiO_2$-based photocatalysts): minimizing photogenerated electron–hole recombination rates and expanding their useful range of operation into visible light wavelengths. Secondary targets include the reduction of crystallite size and the resulting increase in surface area as well as the modification of adsorption properties.

Coupling of semiconductor oxides that show a clear energy difference between their valence bands as well as between their conduction bands (the two differences-shifts being to the same direction) is a common strategy to minimize recombination. The appropriate combinations can easily be predicted by plotting the energy diagrams of the various individual semiconductors (see for example the excellent review of [76]). Also, if one of the semiconductor components has an energy gap small enough to absorb visible light, then its introduction can lead to solar light utilization.

Of particular interest is the coupling of the most common $TiO_2$ catalyst with other semiconductors that have lower valence and conduction band levels ($E_{VB}$ and $E_{CB}$, respectively) with respect to those of $TiO_2$. That leads to electron and hole transfer between the two materials in opposite directions [174] (as shown in Fig. 2 in the case of a $TiO_2$–$WO_3$ system), thus limiting recombination of the photogenerated species in the same material. To that direction, $SnO_2$ (see for example [199,200]), $ZrO_2$ (see for example [201,202]), $MoO_3$ (see for example [203]), $WO_3$ (see for example [203] and more references below), to mention a few materials, have been coupled with $TiO_2$.

Although the photocatalytic treatment of water and air streams using $TiO_2$ has been the subject of ample research during the last three decades, its widespread application is restricted by the necessity of using artificial UV illumination since $TiO_2$ (the most popular photocatalyst) does not show visible light photoactivity. There has therefore been a strong need for the development of visible light-active modifications of $TiO_2$. The most promising of the latter include S, N, or C doping that introduce energy levels within the band gap (see [4,204] and references therein) as well as dye-sensitization [205,206] that was initially developed for solar cell applications [205]. Recently, boron-doped $TiO_2$ is also gaining pace (see for example [206], [207]). Coupling with smaller gap semiconductors can again offer a solution.

As already stated in Section 2.1 above, $WO_3$ is a promising additive for $TiO_2$ since it modifies its photochemical properties in a favourable manner both with respect to reduced recombination and visible light activity. Bicomponent $WO_3$ and $TiO_2$ materials have shown enhanced UV photocatalytic and photoelectrocatalytic activity with respect to their plain component analogues, since their valence and conduction band energy diagrams favour electron injection from the conduction band of $TiO_2$ to that of $WO_3$ and hole transfer between valence bands in the opposite direction. This in turn reduces electron–hole recombination in both semiconductors [41,137,167,186]. However, the effect of $TiO_2$ on visible light

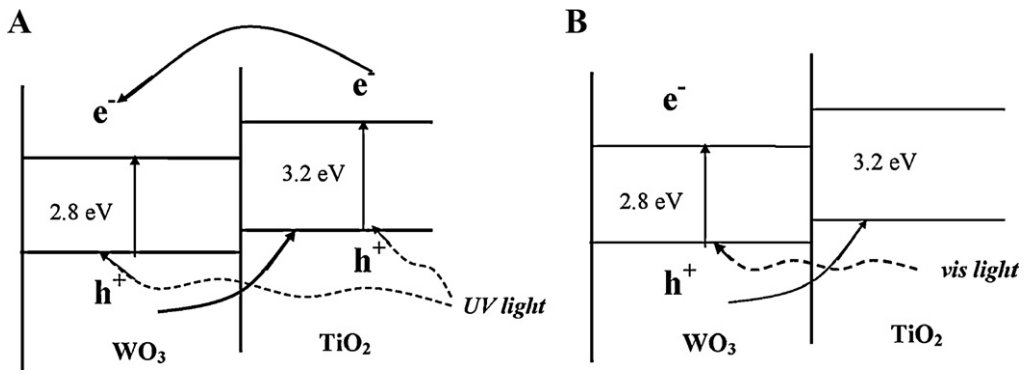


**Fig. 2.** Energy diagram of $WO_3$ and $TiO_2$ materials in contact, showing corresponding valence and conduction band positions as well as hole and electron transfer, during UV (A) and visible (B) light illumination.

excitation of $WO_3$ has only recently been hinted (with respect to resulting photocurrent [168] and hydrophilicity [42]) and there are very few studies on its effect on $WO_3$ visible light catalytic activity towards the bulk oxidation of organics [169,170].

Besides the $TiO_2/WO_3$ anodes there are other semiconductor combinations that have been employed in photoelectrocatalytic water splitting or organics oxidations. For the former application some recent examples include $SnO_2/BiVO_4$ [98], $TiO_2/SrTiO_3$ [71] and $WO_3/BiVO_4$ [74,208] photoelectrodes. For the latter, examples include $TiO_2/SnO_2$ [209], $Cu_2O/TiO_2$ [210], $ZnO/ZnWO_4/WO_3$ [211], $SnO_2/TiO_2$ [97], $Fe_3O_4/WO_3$ [212] and $Bi_2O_3/TiO_2$ [66,100] photoelectrocatalysts.

The main advantage envisaged in using bi-component photoanodes is the possibility of shifting the light absorption spectrum into the visible region, hence making operation under solar radiation viable. The simultaneous reduction of electron–hole recombination rates should be a secondary issue since in photoelectrocatalysis (unlike plain photocatalysis) the application of the external bias largely reduces recombination rates.

## 4. Electrosynthesized-electrodeposited $TiO_2$–$WO_3$ photoanodes for photoelectrocatalysis in aqueous media

### 4.1. Cathodic electrosynthesis/electrodeposition of bicomponent $TiO_2/WO_3$ coatings

The cathodic deposition approaches for both $TiO_2$ and $WO_3$ film preparation of Section 2.2.2.1 have been combined by Rajeswhar, Pauporte, Tacconi and co-workers [165–167,137,186] to produce bicomponent $TiO_2/WO_3$ coatings on optically transparent electrodes and record the photoresponse of small electrodes under UV illumination, in supporting electrolyte solutions or in the presence of simple organics such as formate ions. The expected photocurrent increased due to the semiconductor band coupling and associated recombination reduction described above. They have used both sequential $WO_3$ and $TiO_2$ electrodeposition/electrosynthesis from different solutions under an appropriate constant potential or, mainly, pulsed deposition from a single mixed bath, whereby the potential switched between values favouring $WO_3$ deposition only (less negative) and others that favoured both $WO_3$ and $TiO_2$ deposition (more negative). The former protocol resulted in clearly defined bilayer samples while the latter in a mixed, alternate layers structure.

Georgieva et al. and Valova et al. recently followed the pioneering work of these workers by adopting the sequential deposition protocol [168–170,213–215] and expanded the related studies to:

(i) the use of practical and economical stainless steel substrates,
(ii) the spectroscopic study (energy dispersive spectroscopy (EDS), auger electron spectroscopy (AES) and Raman spectroscopy) of the bi-component catalysts,
(iii) the use of visible light activation,
(iv) the bulk photoelectrolysis of organics in a small batch reactor,
(v) the effect of plating parameters and composition on catalyst morphology and activity.

That work can be viewed as the natural extension of basic research, carried out by Rajeswhar, Pauporte, Tacconi and co-workers, to applied research, aiming at scaling up the process and making it more feasible for practical applications. The following three sections of this review are focused on results obtained in the authors' laboratory, most of which has been presented in References [168–170,213–215].

### 4.2. Microscopic and spectroscopic characterization of photocatalysts: effect of preparation conditions and oxide components loading on coating morphology and local composition

The main morphological feature of electrochemically prepared bi-component $TiO_2/WO_3$ oxides, following temperature annealing in the 300–500 °C range to render them crystalline, is a cracked-mud structure of the underlying $WO_3$ layer which consists of islands-patches a few μm wide (see the SEM image of Fig. 3(A)). The sequential constant potential deposition of $TiO_2$ from a separate bath further covers the $WO_3$ terraces with $TiO_2$ (retaining the overall morphology) but also gives rise to the formation of smaller particles of the new material (Fig. 3(B)). W and Ti elemental X-ray mapping obtained by EDS (Fig. 3(C) and (D)) points to extensive mixing of $WO_3$ and $TiO_2$ (a condition for successful synergism) and that $TiO_2$ is mainly located on island terraces whereas an $WO_3$ underlayer is also present within the cracks (see the tilted "Y" region in the top-right-hand corner of Fig. 3(B)–(D) [170].

The preferential deposition of $TiO_2$ on top of the $WO_3$ islands instead into the cracks can be explained by the easier blanketing of the latter by $H_2$ evolved at the highly negative potential (−2.00 V vs MSE) applied during the cathodic electrosynthesis of $TiO_2$ [168,213].

Sputter-etch AES was employed to perform elemental depth-profiling of the coatings [168]. Fig. 4 shows the results of such experiments at two locations, in the center (A) and the verges (B) of an island (such as those shown in Fig. 3).

Enrichment with $TiO_2$ in the center of the island is confirmed again and gradual sputter-etching of the coating allows for an estimate of the layer thickness. Since 1 min of sputtering under the given conditions corresponded to the etching of approximately 4 nm of material, the thickness of the $TiO_2$ overlayer seems to exceed 400 nm in location (A) whereas it is limited to ca. 160 nm at location (B) and is succeeded by the $WO_3$ underlayer. Nevertheless, both Ti and W elements can be traced (even if at different percentages) in all locations within the 250 nm diameter of the analysis spot, indicating porosity of the overlayer and good component mixing, necessary for synergism.

The effect of $TiO_2$ thickness on coating morphology and photoelectrocatalytic activity has been studied [214]. Fig. 5 shows the back-scattered electron images (BEI) of SEM micrographs for two coatings of different $TiO_2$ loadings over the same $WO_3$ deposit. Bright areas correspond to $WO_3$ and dark areas to $TiO_2$ since the element with a higher atomic mass (i.e. W) backscatters electrons to a larger extent. It can be seen that the coating with the thicker $TiO_2$ overlayer is micro-particulate and rougher. However, the catalyst with the higher $TiO_2$ loading was proven to have inferior UV and similar visible light photocatalytic activity with that of the lower loading, towards the photo-oxidation of chlorophenol. It seems that the increase in catalyst surface area observed at thicker samples is offset by a decrease in the $TiO_2/WO_3$ interfacial area (where synergism is operative) and an increase in ohmic losses within the coating. The optimum Ti:W atomic ratio of these bi-component catalysts was found to be 1:1.

The effect of electrodeposition protocol on $TiO_2/WO_3$ morphology and photoelectrocatalytic activity has also been studied [215]. In more detail, constant potential electrodeposition of $WO_3$ (at −1.0 V vs MSE) in an appropriate bath, followed by constant potential electrosynthesis of $TiO_2$ (at −2.0 V vs MSE) in a second bath, was replaced by pulsed elecrodeposition, performed again in two sequential steps from two different baths. Square waveform pulses were applied on the stainless steel substrate with cathodic pulse potentials of −1.0 V vs MSE for $WO_3$ and −2.0 V vs MSE for $TiO_2$, with a typical pulse duration of 5 ms, followed by a less negative potential pulse at −0.5 V for 5 ms again. The pulse sequence was repeated until the required amount of oxide was deposited.

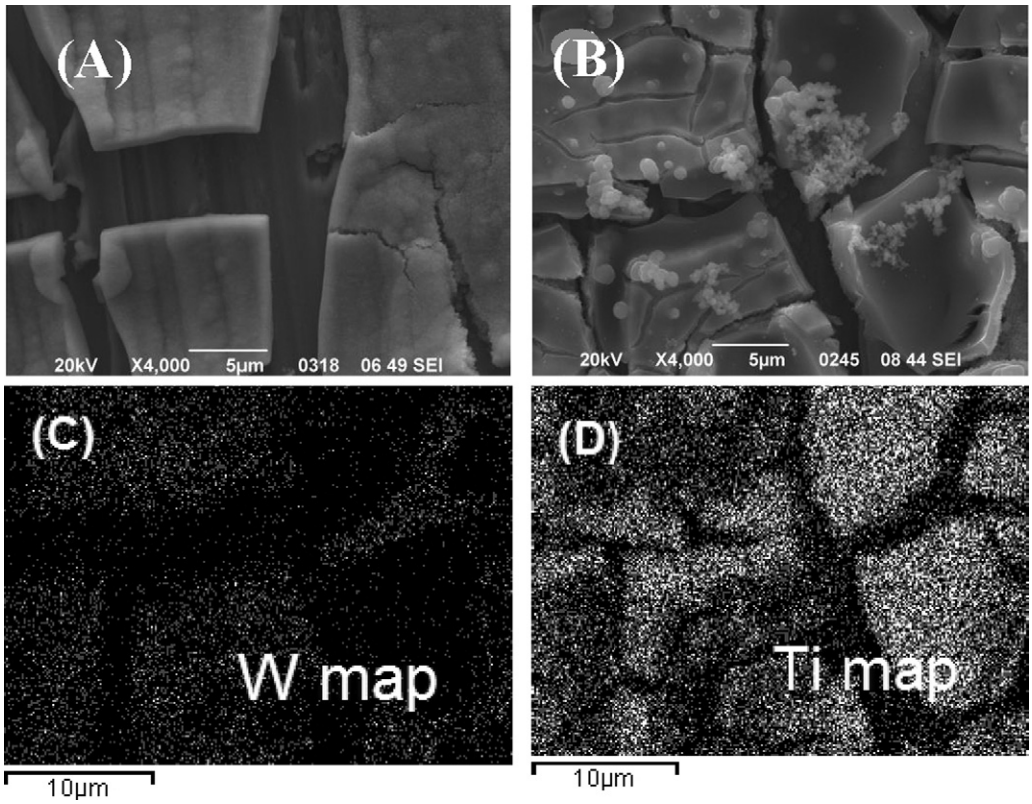


**Fig. 3.** SEM micrographs and EDS maps of electrosynthesized and electrodeposited $WO_3$ and $TiO_2/WO_3$ coatings by cathodic deposition at a stainless steel substrate: (A) SEM (SEI) of a plain $WO_3$ coating (0.83 mg cm$^{-2}$ loading); (B) SEM (SEI) of a $TiO_2/WO_3$ bi-layer coating (0.29 mg cm$^{-2}$ $TiO_2$/0.71 mg cm$^{-2}$ $WO_3$ loading); (C) and (D) EDS mapping for W and Ti, respectively, corresponding to the sample location pictured in (B).

Although the $WO_3$ underlayer obtained by pulsed deposition had a similar morphology to that of the constant potential deposition (albeit slightly smoother and denser, with narrower cracks, than that of Fig. 3(A) above), the $TiO_2$ overlayer had significant differences both in particle size and growth location. Fig. 6 shows SEM micrographs (both in secondary electron imaging, SEI, and back-scattered electron imaging, BEI, modes). It can be seen that $TiO_2$ grows in the form of nanoparticles and preferentially in the cracks of the $WO_3$ underlayer (i.e. in an opposite manner to that observed at constant potential grown deposits). We believe that $TiO_2$ grows preferentially over thin $WO_3$ (or uncovered stainless steel) locations in the cracks since at thicker $WO_3$ locations the latter is not fully reduced during the 5 ms pulse at −2.0 V vs MSE. The facile reduction of $WO_3$ at the highly negative potentials of $TiO_2$ electrosynthesis needs to be completed first, before nitrate reduction/hydrogen evolution–alkalization takes place and leads to $TiO_2$ precipitation.

When the amount of $TiO_2$ deposited by pulse deposition increased, then an overflow of $TiO_2$ particles from the cracks and onto the $WO_3$ terraces occurred, resulting in a cauliflower morphology [215]. The Raman spectrum at various typical locations confirmed the predominance of $TiO_2$ in the cracks and on the surface-topmost locations of the islands and that of $WO_3$ in shallow openings on the islands' flat base [215].

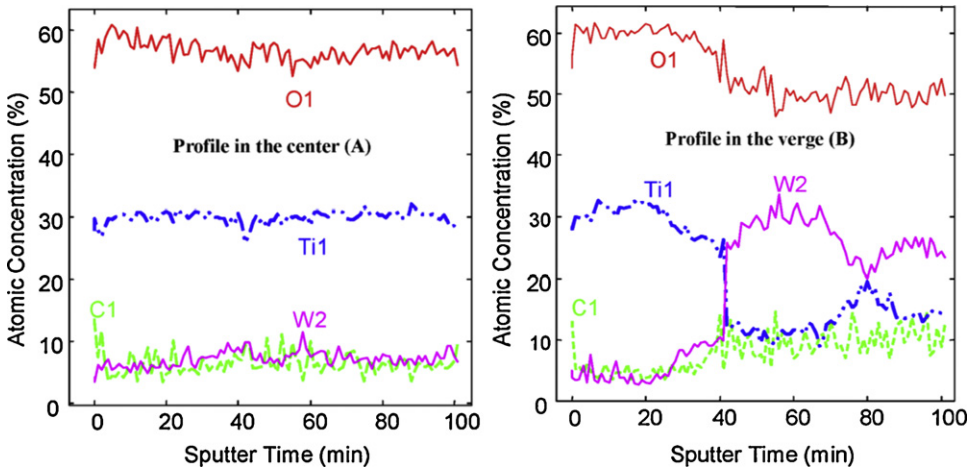


**Fig. 4.** Auger depth profiles of elements at points in the center (A) and at the verges (B) of the deposit islands of a bilayer $TiO_2/WO_3$ sample.

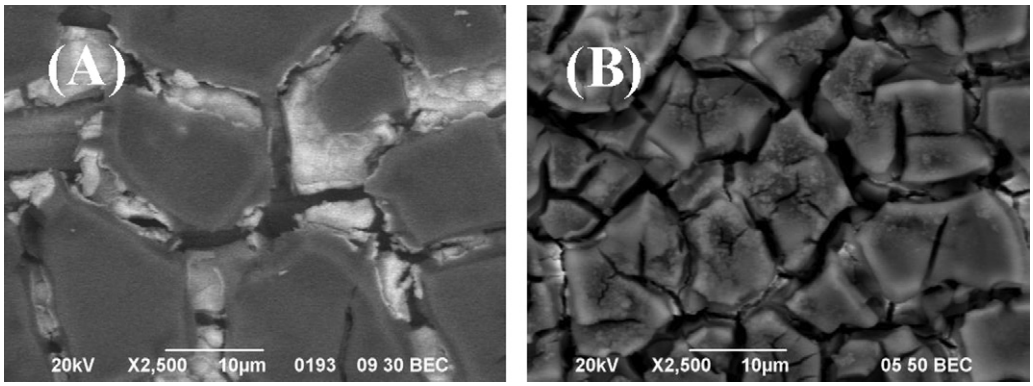


**Fig. 5.** SEM micrographs (BEI) of $TiO_2/WO_3$ coatings: (A) $TiO_2$ (0.30 mg cm$^{-2}$)/$WO_3$ (0.80 mg cm$^{-2}$); (B) $TiO_2$ (0.77 mg cm$^{-2}$)/$WO_3$ (0.80 mg cm$^{-2}$).

Although pulsed electrodeposition allows for a very accurate oxide loading and a nanoparticulate high surface area, no significant increase in photoelectrocatalytic degradation of chlorophenol was found [215], indicating that the increase in surface area is offset by a decrease in the extent and quality of $TiO_2/WO_3$ contact. The best synergism and photoelecrocatalytic activity was therefore observed for thin $TiO_2$ overlayers deposited on the underlying $WO_3$ patches via continuous electrodeposition at a constant potential.

### 4.3. Photoelectrochemical characterization of catalysts

#### 4.3.1. Photovoltammetry

Photovoltammetry at semiconductor electrodes comprises the continuous recording of the current observed under illumination (more accurately, the difference between the dark current and that during exposure to light) as a function of the slowly varied applied potential. It is normally carried out at small photoelectrode specimens under potentiostatic control in three-electrode cells, equipped with a flat quartz window opposite the photoanode (acting as the working electrode). The cell is completed with a reference electrode and a counter/auxiliary electrode. The recorded photocurrent is directly related to the rate of electron and hole photogeneration under the given conditions (since it arises from photogenerated electron flow) but its correlation to the ability of the photoanode to oxidize organic contaminants is not straightforward. The magnitude of the photocurrent in aqueous solutions containing no other species than the inert supporting electrolyte can be safely related to the rate of production of the powerful $OH^{\bullet}$ radicals resulting from water oxidation by the photogenerated holes.

However, whether these radicals are effective in oxidizing organics that may be present in a solution or react with each other to evolve oxygen, depends on the organic and the particular catalyst. Nevertheless, a clear increase of the photocurrent upon addition of a species in a supporting electrolyte solution is a clear indication that the species undergoes direct oxidation by scavenging holes from the valence band itself or/and some of its oxidation products inject electrons in the conduction band which is depleted of electrons due to the external positive bias ("current doubling" effect).

Fig. 7(A) presents photovoltammograms at plain $TiO_2$/SS, $WO_3$/SS and bicomponent $TiO_2/WO_3$/SS photoelectrodes, under UV illumination (UV-A light Radium Ralutec 9 W/78 UV-AA lamp, $\lambda$ = 350–400 nm, $\lambda_{max}$ = 369 nm, 3 mW cm$^{-2}$) in 0.1 M $Na_2SO_4$ solutions (SS stands for the stainless steel substrate). The counter electrode for these small-specimen/photocurrent experiments has been a short Pt wire while a saturated calomel electrode (SCE) or a Ag/AgCl in KCl electrode were employed as reference electrodes. The shape of the curves is typical of n-type semiconductor behaviour with currents tending to a limiting value at sufficiently positive potentials due to charge carrier transport control. When the semiconductor film is continuous and thick enough then, according to classic n-type semiconductor theory [216,217], a space charge layer is developed within the film (associated with upward bending of the valence and conduction bands as depicted in Fig. 1) and the anodic current that flows through the photoanode is controlled at sufficiently high overpotentials by the migration of the minority carriers (in the case of an n-type semiconductor, the holes) through that space charge region under the influence of the associated electric field. On the contrary, when the catalyst is of a nano-particulate form and hence a space charge region cannot

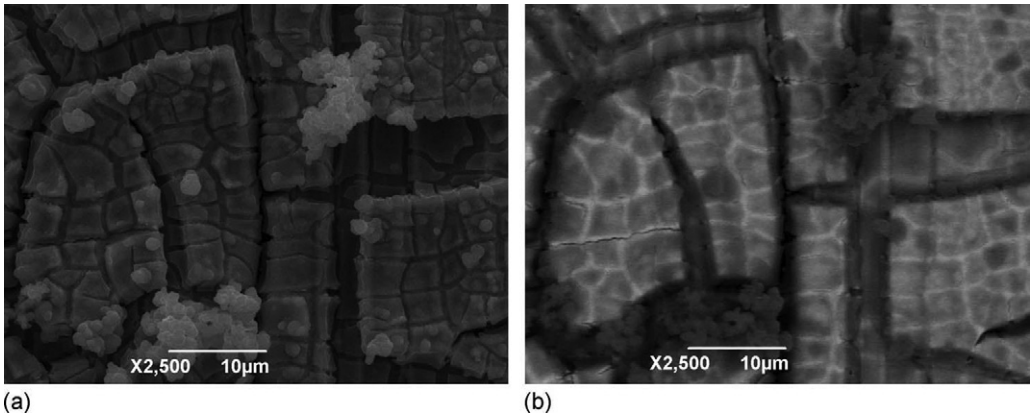


**Fig. 6.** SEI (a)-left and BEI (b)-right SEM micrographs of a pulse-plated. $TiO_2/WO_3$ sample with a loading of 0.35 $TiO_2$/0.82 $WO_3$ mg cm$^{-2}$.

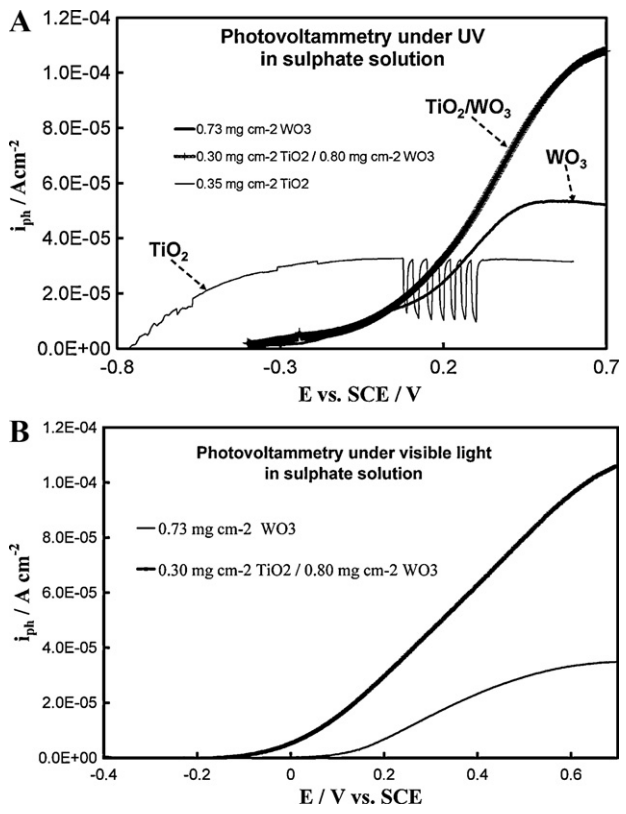


**Fig. 7.** Photovoltammograms (recorded at a 10 mV $s^{-1}$ potential sweep rate towards positive potentials) of $TiO_2$ (0.35 mg $cm^{-2}$)/SS, $WO_3$ (0.73 mg $cm^{-2}$)/SS and $TiO_2$ (0.30 mg $cm^{-2}$)/SS, $WO_3$ (0.80 mg $cm^{-2}$)/SS photoelectrodes, under (A) UV and (B) visible light illumination in 0.1 M $Na_2SO_4$ solutions (SS stands for the stainless steel substrate).

develop within each nanoparticle, the photocurrent is controlled by diffusion of photogenerated electrons through the particle layer [218–221]. In the former case, based on the Gardner model for semiconductor electrodes [222] and the resulting Butler equation [223], the plot of the square of photocurrent vs applied potential ($i_{ph}^2$ vs $E$) is expected to be linear (in the rising part of the photo-voltamogram) if the semiconductor layer is thick enough for a depletion layer to be developed. Since such plots at the foot of the photovoltammetric waves were found to be linear for not heavily doped electrosynthesized/electrodeposited $TiO_2$ and $WO_3$ layers [168,213], it follows that the islands of the semiconductor deposits (see Figs. 3 and 5) must be thick enough for a depletion layer to be formed and the current to be controlled by hole migration across that. A comparison of the photovoltammetry under UV for the three electrodes clearly shows that the onset potential of the $TiO_2$ photoanode is significantly lower than that of the $TiO_2/WO_3$ and $WO_3$ photoanodes, in line with the flat band potential ($E_{fb}$) of the former known to be lower from the one reported for the latter [216]. The most interesting feature of these photovoltammograms is however the much higher limiting photocurrent observed at the bicomponent $TiO_2/WO_3$ electrode, suggesting lower electron–hole recombination rates and indicating a potentially higher photoelectrocatalytic activity of the material towards organics oxidation, when a sufficient positive bias is applied.

Fig. 7(B), showing photovoltamograms under visible light illumination (Radium Ralutec 9 W/71 visible light lamp, $\lambda > 400$ nm, $\lambda_{max} = 437$ nm, 3 mW $cm^{-2}$), points to an unexpected $WO_3$ photocurrent enhancement in the presence of the visible light inactive $TiO_2$. First of all, efficient visible light absorbance by $WO_3$ can only be understood if either the $TiO_2$ overlayer is thin enough to be transparent to visible light or microporous (at least at locations); AES analysis and EDS X-ray mapping (see above) do not exclude these possibilities. Once the underlying or neighbouring $WO_3$ is photoactivated by visible light then its photogenerated holes are transferred to the valence band of $TiO_2$, where they oxidize water to $OH^\bullet$ at the electrode surface (see energy diagram of Fig. 2 (B)). An equivalent representation of the situation, perhaps more appropriate since $TiO_2$ has no significant semiconductor conductivity under visible light illumination, may be the equivalent electron transfer from the $TiO_2$ valence band to $WO_3$ with simultaneous electron transfer from solution oxidizable species to $TiO_2$. (This electron transfer process occurring in effect from solution species to $WO_3$ may be mediated by the presence of a Ti(III)/Ti(IV) couple.)

The effect of the presence of organics in photovoltammetry can reveal the possible mechanism of oxidation of these species at the corresponding photoanode materials. Photovoltammograms of $WO_3$ and $TiO_2/WO_3$ photoelectrodes under UV illumination in $Na_2SO_4$ solutions with and without oxalate or 4-chlorophenol (these being typical organics) were presented in [168–170,213,214]. These revealed that the effect of chlorophenol on the photocurrent was insignificant, indicating that this species is not an efficient direct hole scavenger and could only undergo indirect photooxidation by $OH^\bullet$ radicals produced by hole scavenging by water molecules. On the other hand, the addition of oxalate resulted in a large photocurrent enhancement, characteristic of direct hole scavenging by oxalate which is further enhanced by the "current doubling" effect whereby electron injection by the initial oxidation product to the conduction band of the photocatalyst takes place. The enhancement of the photocurrent when passing from supporting electrolyte (sulphate solution) to an oxalate solution, is more pronounced in the case of the plain $WO_3$/SS electrode, indicating that the recombination rates are higher at this material than at the bilayer $TiO_2/WO_3$/SS one, making the need of an effective hole scavenger more important. Photovoltammograms of plain and bi-layer samples in the same solutions but under visible light (vis) illumination ($\lambda > 400$ nm) revealed similar trends to those observed under UV light [168–170,213,214]. The overall voltammetric picture indicated that in the case of the effective oxalate scavenger, there is no significant difference in photocurrents under UV illumination and only a moderate enhancement under visible light illumination when one passes from plain to bi-layer samples. In the case of 4-chlorophenol however, which is more difficult to oxidize and, due to its indirect oxidation mechanism, cannot limit recombination rates, the $TiO_2/WO_3$ combination has a pronounced effect in increasing the photocurrent.

#### 4.3.2. Bulk photoelectrolysis of dissolved organics

As stated above, photovoltammetry at small photoanode electrodes can only provide an indication of the photoactivity of a material. Hence, prolonged constant potential experiments at larger photoanodes and larger solution volumes (bulk photoelectrolysis) are needed to access the photoelectrocatalytic activity of a semiconductor towards the oxidation of an organic species. It should be noted that although bulk photoelectrolysis of various organics (including microorganisms) on single component $TiO_2$ photoanodes has frequently been used (see for example [8–15,17–24], very few such experiments at $WO_3$ electrodes (under both UV and visible light irradiation) have been reported [16,47,169,170,214,215], whereas bulk photoelectrolysis experiments at bicomponent semiconductor electrodes are also scarce [66,67,73,169,170,214,215].

Examples of the methodology used to assess the photocatalytic and photoelectrocatalytic activity of semiconductor electrodes towards typical organics oxidation are presented in the case of $TiO_2/WO_3$ bicomponent photoanodes in references [169,170,214,215] for the case of the standard organic

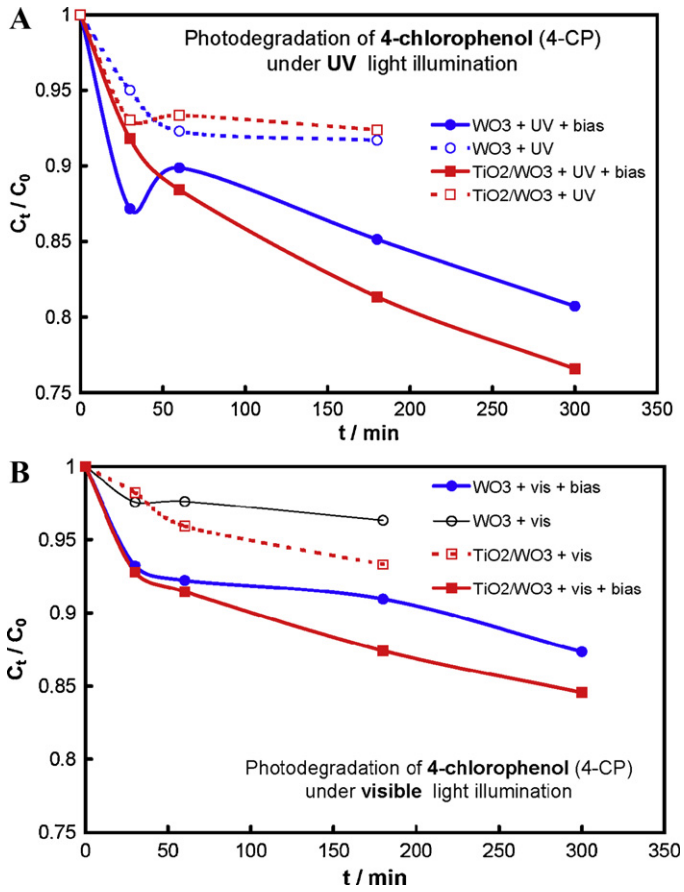


**Fig. 8.** Variation of 4-chlorophenol concentration with time from $10^{-3}$ M 4-chlorophenol + 0.1 M $Na_2SO_4$ 250 ml solutions, during constant potential (+0.4 V vs SCE) photoelectrolysis at large (30 $cm^2$) $WO_3$/SS and $TiO_2$–$WO_3$/SS electrodes, under UV (A) and visible (B) light illumination. Final concentration decreases in the order of: $TiO_2/WO_3 \approx WO_3 > WO_3$ + bias > $TiO_2/WO_3$ under UV light (A) and $WO_3 > TiO_2/WO_3 > WO_3$ + bias > $TiO_2/WO_3$ under visible light (B).

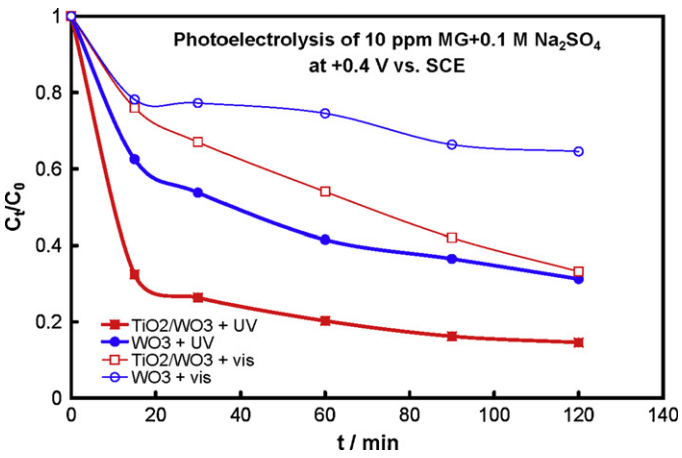


**Fig. 9.** Variation of malachite green (MG) concentration with time from 10 ppm MG + 0.1 M $Na_2SO_4$ 250 ml solutions, during constant potential (+0.4 V vs SCE). Final concentration decreases in the order of $WO_3$ + visible > $TiO_2/WO_3$ + visible ≈ $WO_3$ + UV > $TiO_2/WO_3$ + UV.

pollutant of 4-chlorophenol (4-CP) [170,214,215] and the typical dye of malachite green (MG) [169]. In those works constant potential bulk photoelectrocatalytic experiments were carried out, using electrodes in the 30 $cm^2$ range and 250 ml 0.1 M $Na_2SO_4$ + $10^{-3}$ M 4-CP or 0.1 M $Na_2SO_4$ + 10 ppm MG solutions. The potential was kept constant at +0.4 V vs a saturated calomel (reference) electrode (SCE). To study the effect of applied potential, experiments without the application of an external bias were also performed.

Fig. 8 presents results for 4-CP degradation, under UV (A) or visible (B) light illumination, in the presence or absence of a voltage bias, at both plain $WO_3$ and bicomponent $TiO_2/WO_3$ electrodes (with the counter electrode being a long stainless steel coil and the reference electrode a SCE).

Two general remarks can be readily made. First, there is a pronounced beneficial effect of the applied potential on the photocatalytic activity of both materials. This is important for the effective use of supported photocatalysts since, when compared to their slurry analogues, they have a limited surface area and are prone to mass transport limitations and rapid contamination/deactivation. It becomes even more critical in the case of coatings which are not micro-particulate as typical $TiO_2$ layers prepared from powder catalysts and hence they posses a relatively smaller area and are even more prone to deactivation (as is indeed the case of unbiased samples where there is no organic species removal beyond a certain point). Second, the trends reported and interpreted above for the photocurrents at the plain and bi-component samples are in general translated into similar trends for the photoelectrocatalytic oxidation of 4-CP. That is, the bi-layer $TiO_2/WO_3$/SS photoelectrodes exhibit in all cases superior organics degradation performance when compared to plain $WO_3$/SS photoelectrodes. To quantify the efficient use of the photocurrent for the degradation of organics one should estimate the faradaic efficiency of 4-CP removal at the photoelectrodes. This can be done by calculating the charge passed during the reaction period (by integrating the corresponding photocurrent vs time curves) and comparing it with the charge associated to the photooxidation of these species (estimated by their actual concentration change and applying Faraday's law, assuming that one photogenerated electron–hole pair is needed to initiate the photodegradation process). The faradaic efficiency represents that part of the photocurrent which is used for the organics oxidation (the rest may result in water photooxidation at the anode). Values of 34% and 23% were estimated for $WO_3$ and $TiO_2/WO_3$ respectively under UV light illumination; these values became 68% and 34% under visible light. It can be seen that despite the fact that the bilayer $TiO_2/WO_3$ electrodes are more active than $WO_3$ in removing 4-chlorophenol, the plain $WO_3$ electrodes are characterized by a more effective use of the photocurrent. This in turn means that at $TiO_2/WO_3$ electrodes the rate of concurrent reactions (such as oxygen evolution from the reaction of $OH^\bullet$ radicals with each other) is higher.

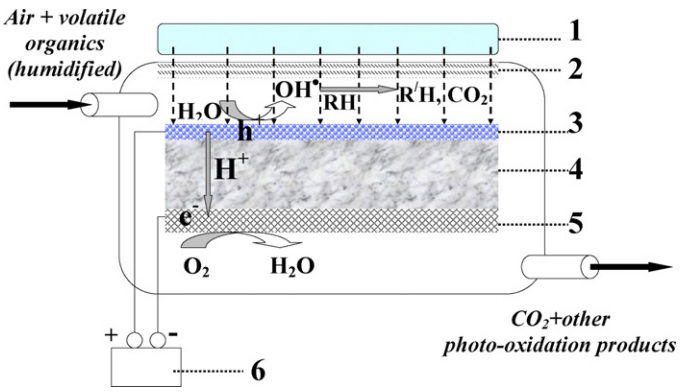


**Fig. 10.** Schematic diagram of a photoreactor for photoeletcrochemical air-treatment. (1) Light source (UV or visible light lamp); (2) transparent window; (3) porous photocatalyst layer (powder catalyst or mesh-supported catalyst); (4) solid polymer electrolyte; (5) porous cathode; (6) power supply.

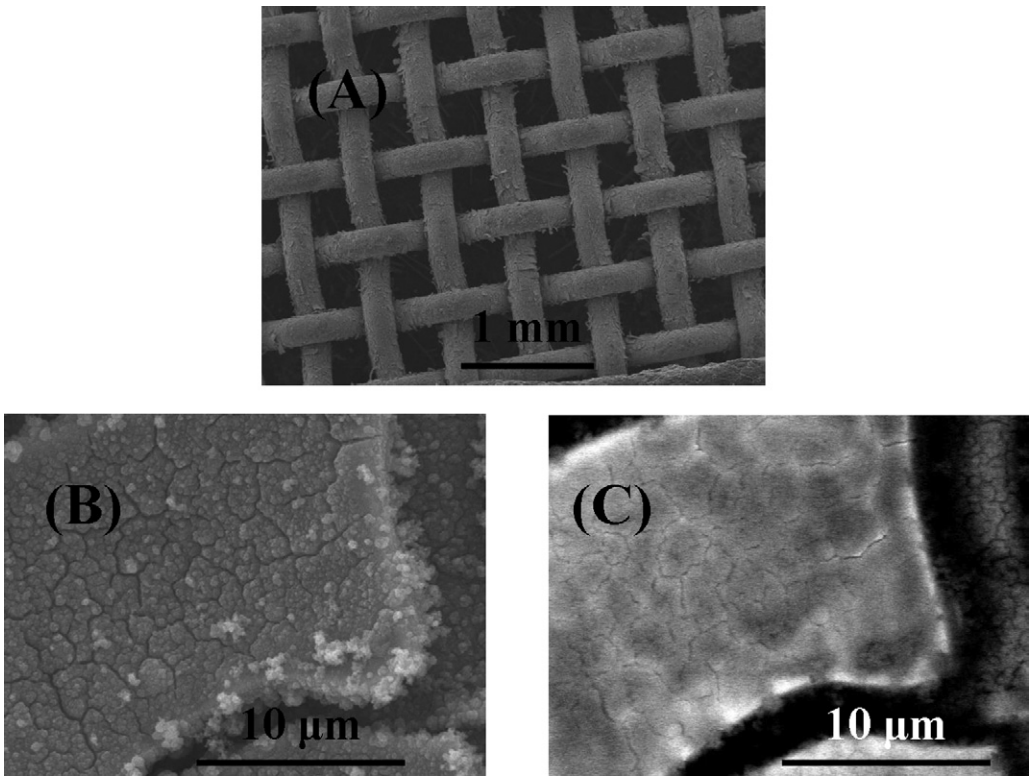


**Fig. 11.** SEM micrographs of (A) a $TiO_2/WO_3$ coated stainless steel mesh; (B) a detail of (A); (C) same as (B) but obtained in a BEI mode.

Fig. 9 presents results for the photodegradation of MG under UV and vis light illumination for 2 h. It can be seen that the UV photoelectrocatalytic activity is always better than the visible one and the bi-layer $TiO_2$–$WO_3$ electrodes are by far superior to their plain $WO_3$ analogues. In more detail, an 85.5% removal of MG was achieved under 2 h UV illumination (resulting in visible solution decolorization), with a 74% removal achieved after just 30 min. Despite being slower (only 33% removal after 30 min), dye removal under vis illumination also reached a significant 66.8% value after 2 h.

## 5. Bi-layer $TiO_2$–$WO_3$ and powder $TiO_2 + WO_3 + C$ photoanodes for the photoelectrocatalytic oxidation of organic vapours in all-solid cells

As already stated in the last paragraph of the Introduction, there are hardly any papers on the photoelectrocatalytic oxidation of gaseous organics within the scope of air treatment applications [11,33–35,224]. This is surprising since both the polymer electrolyte membrane (PEM) fuel cell technology of all-solid electrochemical cells is well developed and the use of solid polymer

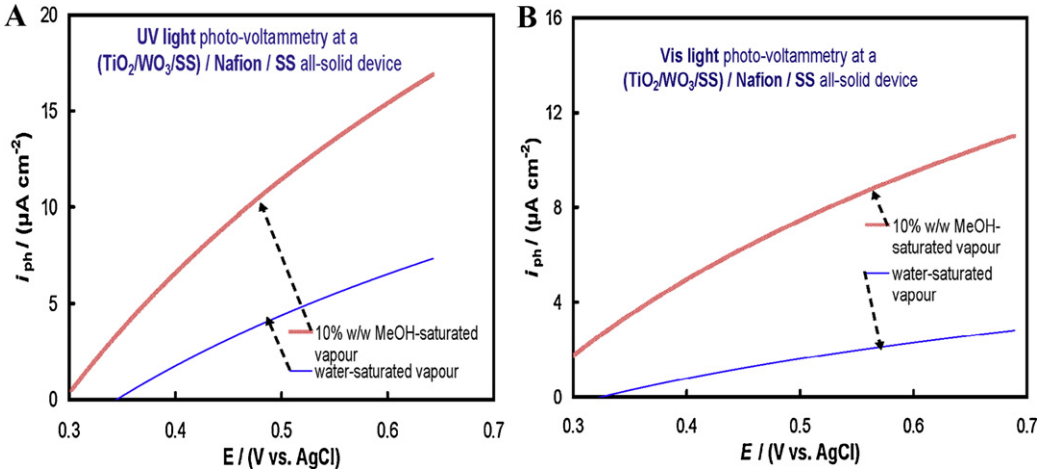


**Fig. 12.** Photovoltammograms (recorded at a 10 mV $s^{-1}$ potential sweep rate towards positive potentials) at electrosynthesized/electrodeposited $TiO_2/WO_3$/SS photoanodes, obtained at a Nafion®-based all-solid cell in the presence of water- and 10% (w/w) methanol solution-saturated vapours, under (A) UV and (B) visible light illumination. Higher photocurrents correspond to the presence of methanol vapours.

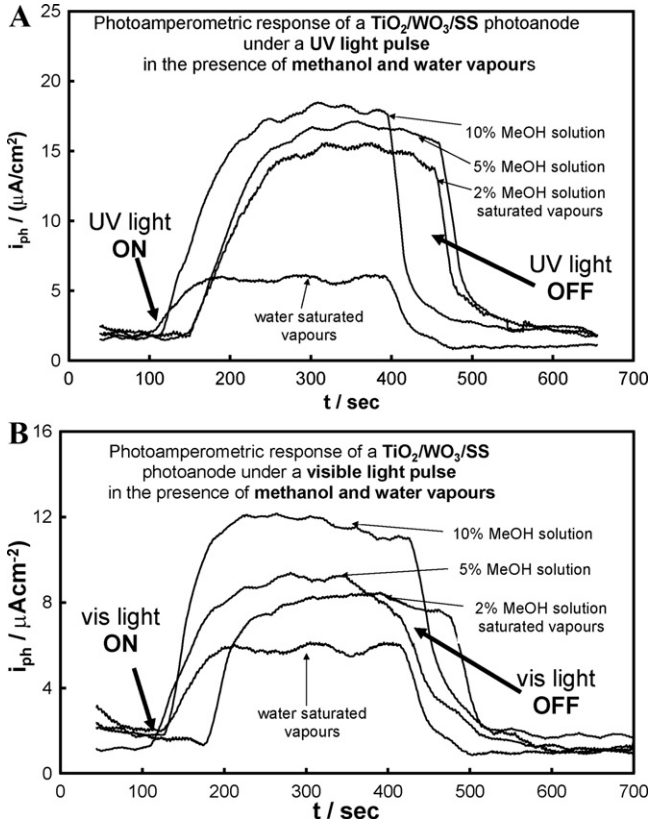


**Fig. 13.** Photoamperometry (photocurrent vs time curves) at electrosynthesized/electrodeposited $TiO_2/WO_3$/SS photoanodes biased at +0.50 V vs Ag/AgCl in a Nafion®-based all-solid cell, in the presence of water and methanol vapours, under (A) UV and (B) visible light illumination. Maximum photocurrents increase in the order of: pure water < 2% (w/w) methanol < 5% (w/w) methanol < 10% (w/w) methanol solution-saturated vapours.

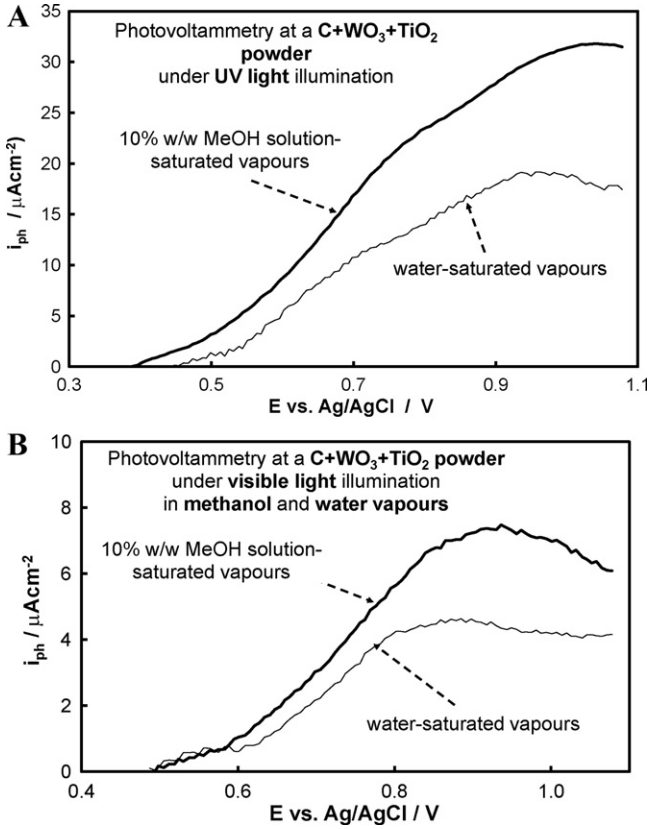


**Fig. 14.** Photovoltammograms (recorded at a 10 mV $s^{-1}$ potential sweep rate towards positive potentials) at mixed $TiO_2 + WO_3 + C$ (+Nafion®) powder-photoanodes, obtained in a Nafion®-based all-solid cell in the presence of water- and 10% (w/w) methanol solution-saturated vapours, under (A) UV and (B) visible light illumination.

electrolyte (SPE) or gel electrolytes in $TiO_2$-based solar cells has recently advanced significantly.

The schematic diagram of the concept of a photoelectrochemical cell and reactor for air treatment is shown in Fig. 10. The proof-of-concept for such an approach was presented in [33,35] whereas the optimisation of the powder photoanodes of [35] has recently been reported in [224].

The photoanode used in [33] was a bilayer $TiO_2/WO_3$ coating electrosynthesized on a stainless steel mesh (see Fig. 11). The open structure of the coated stainless steel substrate (Fig. 11(A)) is necessary for an increased gas/polymer electrolyte/photoelectrocatalyst interface, the locus of the photooxidation process in such a cell. (One should also notice in the back-scattered electron image (BEI) of Fig. 11 (C)) the very thin $TiO_2$ overlayer, depicted as a grey film over the brighter $WO_3$ island.) In the construction of the small demonstration cell, the polymer electrolyte (Nafion®) was supported on a microporous (0.45 μm) HT Tuffryn polysulfone membrane, impregnated with a solution of the polymer and then left to dry. The photoanode mesh and a stainless steel cathode mesh were adhered on opposite faces of the membrane with a quantity of the electrolyte solution (upon drying). A Ag/AgCl wire, served as the reference electrode and was attached (again with the help of a Nafion® solution) on one face of the membrane.

Fig. 12 presents photovoltammograms at such electrosynthesized/electrodeposited $TiO_2/WO_3$/SS photoanodes in a Nafion®-based cell, in the presence of water and methanol vapours (equilibrated with a 10% (w/w) methanolic solution), under UV and visible light illumination.

A continuous rise in the photocurrent with applied potential can be seen (with no clear plateau observed), indicating photocurrent control via photogenerated hole transfer through a developed depletion layer within the thick semiconductor patches [222,223]. The increased response upon addition of methanol points to its direct photooxidation.

Fig. 13 presents results of constant potential amperometry (at +0.5 V vs Ag/AgCl) obtained with the same devices in streams of different methanol content, upon switching on and off the irradiation. It can be seen that there is a continuous increase of the photocurrent as methanol concentration increases but there is gradual current saturation too. The latter is typical of the kinetics of the photoelectrocatalytic oxidation of methanol following a Langmuir–Hinselwood formalism [33].

In search for a more practical photoanode, compatible with fuel cell active electrode layer technology and having a higher surface area a $TiO_2$/C powder mixture (bound with Nafion®) was introduced in [35] and various $WO_3 + TiO_2$/C powder mixture formulations were tried in [224]. The catalytic photoanode coating consists of different size particles and agglomerates of C, $WO_3$ and $TiO_2$, dispersed as mixtures in a solidified Nafion® matrix, pasted on one side of the membrane and left to dry.

Following experimentation with various $WO_3$:$TiO_2$:C ratios [224] it was found that the optimum photoanode composition, for good performance both under UV and visible light, was a 1:2 ratio of W:Ti (atomic) and a 1:2 ratio of C:photocatalyst (w/w) (all electrodes had a 30% (w/w) Nafion® content). Fig. 14 presents the results of photovoltammetry obtained at all-solid photoelectrochemical cells with a mixed $C + TiO_2 + WO_3$ powder photoanode

(0.5 mg $cm^{-2}$ C and 0.9 mg $cm^{-2}$ $TiO_2$ + $WO_3$ with a 1:2 W:Ti atomic ratio formulation), under UV and visible light illumination in water and methanol vapours. S-shaped curves are observed, with the clear signs of a photocurrent plateau (as opposed to the ill-defined rise in Fig. 12) being characteristic of photocurrent control by photogenerated electron transfer through a nanoparticulate film [218–221]. Again, the photocurrent rises in the presence of methanol, indicating a direct hole-methanol reaction. Constant potential experiments at varied methanol levels revealed a picture similar to that of Fig. 13.

## 6. Conclusions – future directions

The use of electrochemical enhancement in the photooxidation of organic pollutants at supported semiconductor catalysts becomes an option in cases that supported catalysts are required, either due to catalyst management considerations, need for modular photoreactor design or application to air-treatment.

Although there have been many studies on photoelecrochemical water treatment, the technology has not yet been commercialised, perhaps due to the complexity and cost of setting up and operating an electrochemical cell as well as to the fact that it has not yet provided significant enhancement in universal organic load removal. The technique seems to work well for specific contaminants (some dyes, microbes, etc.) but with moderate success on standard pollutants such as 4-chlorophenol. Although photoelectrocatalysis at supported photoanodes is unlikely to replace at this stage the use of photocatalyst powders in a slurry form, we believe that it can still find application in small volume (and organic load) water treatment such as potable water disinfection at domestic outlets or personal water supplies.

The use of bi-component semiconductor oxide anodes can significantly improve the photooxidation efficiency and (if the materials are appropriately coupled) the usage of the visible part of the solar light too. Among the few systems studied, bi-component $TiO_2$ and $WO_3$ photocatalytic coatings can lead to very efficient and practical photoanodes. Following the pioneering work of Hepel and co-workers as well as that of Rajeshwar and co-workers, who used bi-component $TiO_2/WO_3$ catalytic coatings prepared electrochemically in the photoelectrocatalytic oxidation of organics, Georgieva et al. have recently explored issues of the related research that could increase the potential of these materials for practical applications. To that direction, we believe that their main contribution has been the use of practical stainless steel substrates and the operation of the $TiO_2/WO_3$ catalysts under visible light illumination. Research into more active semiconductor oxide formulations (e.g. incorporation of $Bi_2O_3$, $BiVO_4$, $SrTiO_3$) should be further explored.

With respect to possible future process modifications we can mention here at least two research avenues; one for water treatment and one for gas treatment. In the former case, it would be worth investigating the application of electrochemical enhancement at powder semiconductor oxide slurries if these are turned into a fluidized bed electrode with the addition of small quantities of carbon powders (to increase conductivity) and current collector rods. On the other hand, in the case of air treatment, a stainless steel base (that could serve as a counter electrode), with a Nafion® membrane or film above it and the photocatalyst spread on the outer face of the membrane/film, could be a straightforward modification of already existing photoreactors. We believe that the photoelectrochemical treatment of volatile organic compounds (VOCs), where supported photocatalysts are necessarily used, could offset their limited surface area and high contamination rate, and should become a priority path of future research in the area.

## Acknowledgement

This work was supported by a NATO Science for Peace Project 982835.

## References

[1] M.R. Hoffmann, S.T. Martin, W. Choi, D.W. Bahnemann, Environmental applications of semiconductor photocatalysis, Chem. Rev. 95 (1995) 69–96.
[2] A. Mills, V. Le Hunte, An overview of semiconductor photocatalysis, J. Photochem. Photobiol. A 108 (1997) 1–35.
[3] A. Fujishima, T.N. Rao, D.A. Tryk, Titanium dioxide photocatalysis, J. Photochem. Photobiol. C 1 (2000) 1–21.
[4] X. Chen, S.S. Mao, Titanium dioxide nanomaterials: synthesis, properties, modifications and applications, Chem. Rev. 107 (2007) 2891–2959.
[5] Z. Ding, X. Hu, P.L. Yue, G.Q Lu, P.F. Greenfield, Synthesis of anatase $TiO_2$ supported on porous solids by chemical vapor deposition, Catal. Today 68 (2001) 173–182.
[6] R.W. Matthews, Kinetics of photocatalytic oxidation of organic solutes over titanium dioxide, J. Catal. 111 (1988) 264–272.
[7] S. Nishida-Yamazaki, K.J. Nagano, L.A. Phillips, S. Cervera-March, M.A. Anderson, Photocatalytic degradation of trichloroethylene in the gas phase using titanium dioxide pellets, J. Photochem. Photobiol. A 70 (1993) 95–99.
[8] T. Matsunaga, R. Tomoda, T. Nakajima, H. Wake, Photoelectrochemical sterilization of microbial cells by semiconductor powders, FEMS Microbiol. Lett. 29 (1985) 211–214.
[9] D.H. Kim, M.A. Anderson, Photoelectrocatalytic degradation of formic acid using a porous $TiO_2$ thin-film electrode, Environ. Sci. Technol. 28 (3) (1994) 479–483.
[10] A. Wahl, M. Ulmann, A. Carroy, B. Jermann, M. Dolata, P. Kedzierzawski, C. Chatelain, A. Monnier, J. Augustynski, Photoelectrochemical studies pertaining to the activity of $TiO_2$ towards photodegradation of organic compounds, J. Electroanal. Chem. 396 (1995) 41–51.
[11] O. Enea, A porous cell for photo-assisted electrooxidations in the gas phase, Electrochim. Acta 41 (1996) 473–476.
[12] I.M. Butterfield, P.A. Christensen, T.P. Curtis, J. Gunlazuardi, Water disinfection using an immobilised titanium dioxide film in a photochemical reactor with electric field enhancement, Water Res. 31 (3) (1997) 675–677.
[13] I.M. Butterfield, P.A. Christensen, A. Hamnett, K.E. Shaw, G.M. Walker, S.A. Walker, C.R. Howarth, Applied studies on immobilized titanium dioxide films as catalysts for the photoelectrochemical detoxification of water, J. Appl. Electrochem. 27 (1997) 385–395.
[14] J.A. Byrne, B.R. Eggins, Photoelectrochemistry of oxalate on participate $TiO_2$ electrodes, J. Electroanal. Chem. 457 (1998) 61–72.
[15] P. Fernandez-Ibanez, S. Malato, O. Enea, Photoelectrochemical reactors for the solar decontamination of water, Catal.Today 54 (1999) 329–339.
[16] J. Luo, M. Hepel, Photoelectrochemical degradation of naphthol blue black diazo dye on $WO_3$ film electrode, Electrochim. Acta 46 (19) (2001) 2913.
[17] M.V.B. Zanoni, J.J. Sene, M.A. Anderson, Photoelectrocatalytic degradation of Remazol Brilliant Orange 3R on titanium dioxide thin-film electrodes, J. Photochem. Photobiol. A 157 (1) (2003) 55–63.
[18] P.A. Christensen, T.P. Curtis, T.A. Egerton, S.A.M. Kosa, J.R. Tinlin, Photoelectrocatalytic and photocatalytic disinfection of E. coli suspensions by titanium dioxide, Appl. Catal. B 41 (2003) 371–386.
[19] I. Mintsouli, N. Philippidis, I. Poulios, S. Sotiropoulos, Photoelectrochemical characterisation of thermal and particulate titanium dioxide electrodes, J. Appl. Electrochem. 36 (4) (2006) 463–474.
[20] T.A. Egerton, P.A. Christensen, S.A.M. Kosa, B. Onoka, J.C. Harper, J.R. Tinlin, Photoelectrocatalysis by titanium dioxide for water treatment, Int. J. Environ. Pollut. 27 (1-3) (2006) 2–19.
[21] M. Uzunova, M. Konstantinov, J. Georgieva, C. Dushkin, D. Todorovsky, N. Philippidis, I. Poulios, S. Sotiropoulos, Photoelectrochemical characterisation and photocatalytic activity of composite $La_2O_3$–$TiO_2$ coatings on stainless steel, Appl. Catal. B 73 (1-2) (2007) 23–33.
[22] N. Philippidis, S. Sotiropoulos, A. Efstathiou, I. Poulios, Photoelectrocatalytic degradation of the insecticide imidacloprid using $TiO_2$/Ti electrodes, J. Photochem. Photobiol. A 204 (2-3) (2009) 129–136.
[23] L.E. Fraga, M.A. Anderson, M.L.P.M.A. Beatriz, F.M.M. Paschoal, L.P. Romão, M.V.B. Zanoni, Evaluation of the photoelectrocatalytic method for oxidizing chloride and simultaneous removal of microcystin toxins in surface waters, Electrochim. Acta 54 (7) (2009) 2069–2076.
[24] N. Philippidis, E. Nikolakaki, S. Sotiropoulos, I. Poulios, Photoelectrocatalytic inactivation of *E. coli* XL-1 blue colonies in water, J. Chem. Technol. Biotechnol. 85 (8) (2010) 1054–1060.
[25] A. Patsoura, D. Kondarides, X.E. Verykios, Photocatalytic degradation of organic pollutants with simultaneous production of hydrogen, Catal. Today 124 (3-4) (2007) 94–102.
[26] J.A. Byrne, A. Davidson, P.S.M. Dunlop, B.R. Eggins, Water treatment using nano-crystalline $TiO_2$ electrodes, J. Photochem. Photobiol. A 148 (1–3) (2002) 365–374.
[27] J. Shang, S. Xie, T. Zhu, J. Li, Solid-state, planar photoelectrocatalytic devices using a nanosized $TiO_2$ layer, Environ. Sci. Technol. 41 (2007) 7876.
[28] A.F. Nogueira, C. Longo, M.-A. De Paoli, Polymers in dye sensitized solar cells: overview and perspectives, Coord. Chem. Rev. 248 (2004) 1455.

[29] E. Stathatos, P. Lianos, Increase of the efficiency of quasi-solid state dye-sensitized solar cells by a synergy between titania nanocrystallites of two distinct nanoparticle sizes, Adv. Mater. 19 (2007) 3338–3341.
[30] S. Ichikawa, R. Doi, Hydrogen production from water and conversion of carbon dioxide to useful chemicals by room temperature photoelectrocatalysis, Catal. Today 27 (1996) 271.
[31] S. Ichikawa, Chemical conversion of carbon dioxide by catalytic hydrogenation and room temperature photoelectrocatalysis, Energy Convers. Manage. 36 (6–9) (1995) 613.
[32] B. Seger, P.V. Kamat, Fuel cell geared in reverse: photocatalytic hydrogen production using a $TiO_2$/Nafion/Pt membrane assembly with no applied bias, J. Phys. Chem. C 113 (43) (2009) 18946.
[33] J. Georgieva, S. Armyanov, I. Poulios, S. Sotiropoulos, An all-solid photoelectrochemical cell for the photooxidation of organic vapours under ultraviolet and visible light illumination, Electrochem. Commun. 11 (2009) 1643.
[34] S.-Y. Ye, Q.-M. Tian, X.-L. Song, S.-C. Luo, Photoelectrocatalytic degradation of ethylene by a combination of $TiO_2$ and activated carbon felts, J. Photochem. Photobiol. A 208 (2009) 27–35.
[35] J. Georgieva, S. Armyanov, I. Poulios, A.D. Jannakoudakis, S. Sotiropoulos, Gas phase photoelectrochemistry in a polymer electrolyte cell with a titanium dioxide/carbon/nafion photoanode, Electrochem. Solid-State Lett. 3 (10) (2010) 11–13.
[36] N. Serpone, E.V. Emeline, Fundamentals in metal-oxide heterogeneous photocatalysis, in: M.D. Archer, A.J. Nozik (Eds.), Nanostructured and Photoelectrochemical Systems for Solar Photon Conversion, Imperial College Press, London, 2008, pp. 275–392.
[37] K. Hashimoto, H. Irie, A. Fujishima, $TiO_2$ photocatalysis: a historical overview and future prospects, Jpn. J. Appl. Phys. 44 (2005) 8269–8285.
[38] V. Augugliaro, L. Palmisano, A. Sclafani, M. Schiavello, Activity of chromium-ion-doped titania for the dinitrogen photoreduction to ammonia and for the phenol photodegradation, J. Phys. Chem. 92 (1988) 6710–6713.
[39] S. Sakthivel, B. Neppolian, B. Arabindoo, M. Palanichamy, V. Murugesan, $TiO_2$ catalysed photodegradation of leather dye, Acid Green 16, J. Sci. Ind. Res. 59 (2000) 556–562.
[40] P. Reeves, R. Ohlhausen, D. Sloan, K.T. Scoggins, C. Clark, B. Hutchinson, D. Green, Photocatalytic destruction of organic dyes in aqueous $TiO_2$ suspensions using concentrated simulated and natural solar energy, Sol. Energy 48 (1992) 413–420.
[41] T. He, Y. Ma, Y. Cao, X. Hu, H. Liu, G. Zhang, W. Yang, V. Yao, Photochromism of $WO_3$ colloids combined with $TiO_2$ nanoparticles, J. Phys. Chem. B 106 (2002) 12670–12676.
[42] V. Miyauchi, A. Nakajima, T. Watanabe, V. Hashimoto, Photoinduced hydrophilic conversion of $TiO_2$/$WO_3$ layered thin films, Chem. Mater. 14 (2002) 4714–4720.
[43] M. Gillet, V. Aguir, V. Lemire, V. Gillet, V. Schierbaum, The structure and electrical conductivity of vacuum-annealed $WO_3$ thin films, Thin Solid Films 467 (2004) 239–246.
[44] V. Shiyanovskaya, M. Hepel, Bicomponent $WO_3$/$TiO_2$ films as photoelectrodes, J. Electrochem. Soc. 146 (1999) 243–249.
[45] V. Kopp, B.N. Harmon, S.H. Liu, Band structure of cubic $Na_xWO_3$, Solid State Commun. 22 (1977) 677–679.
[46] T. Ohno, F. Tanigawa, K. Fujihara, S. Izumi, M. Matsumura, Photocatalytic oxidation of water on $TiO_2$-coated $WO_3$ particles by visible light using Iron(III) ions as electron acceptor, J. Photochem. Photobiol. A 118 (1998) 41–44.
[47] M. Hepel, J. Luo, Photoelectrochemical mineralization of textile diazo dye pollutants using nanocrystalline $WO_3$ electrodes, Electrochim. Acta 47 (2001) 729–740.
[48] C. Santato, M. Ulmann, J. Augustynski, Photoelectrochemical properties of nanostructured tungsten trioxide films, J. Phys. Chem. B 105 (2001) 936–940.
[49] I. Poulios, I. Tsachpinis, Photodegradation of the textile dye Reactive Black 5 in the presence of semiconducting oxides, J. Chem. Technol. Biotechnol. 74 (1999) 349–357.
[50] I. Poulios, A. Avranas, E. Rekliti, A. Zouboulis, Photocatalytic oxidation of Auramine O in the presence of semiconducting oxides, J. Chem. Technol. Biotechnol. 75 (2000) 205–212.
[51] S. Sakthivel, B. Neppolian, M.V. Shankar, B. Arabindoo, M. Palanichamy, V. Murugesan, Solar photocatalytic degradation of azo dye: comparison of photocatalytic efficiency of ZnO and $TiO_2$, Sol. Energy Mater. Sol. Cells 77 (2003) 65–82.
[52] E.M. Kaidashev, M. Lorenz, H. Wenckstern, A. Rahm, H.C. Semmelhack, K.H. Han, G. Benndorf, C. Bundesmann, H. Hochmuth, M. Grundmann, High electron mobility of epitaxial ZnO thin films on c-plane sapphire grown by multistep pulsed-laser deposition, Appl. Phys. Lett. 82 (2003) 3901.
[53] U. Ozgur, Y.I. Alivov, C. Liu, A. Teke, M.A. Reshchikov, S. Dogan, V. Avrutin, S.J. Cho, H. Morkoc, A comprehensive review of ZnO materials and devices, J. Appl. Phys. 98 (4) (2005) 1–103.
[54] T. Minami, H. Tanaka, T. Shimakawa, T. Miyata, H. Sato, High-efficiency oxide heterojunction solar cells using $Cu_2O$ sheets, Jpn. J. Appl. Phys. 43 (2004) L917–L919.
[55] A.A. Ogwu, E. Bouquerel, O. Ademosu, S. Moh, E. Crossan, F. Placido, The influence of rf power and oxygen flow rate during deposition on the optical transmittance of copper oxide thin films prepared by reactive magnetron sputtering, J. Phys. D: Appl. Phys. 38 (2005) 266–271.
[56] N. Serin, T. Serin, S. Horzum, Y. Celik, Annealing effects on the properties of copper oxide thin films prepared by chemical deposition, Semicond. Sci.Technol. 20 (2005) 398.
[57] M. Izaki, T. Shinagawa, K.T. Mizuno, Y. Ida, M. Inaba, A. Tasaka, Electrochemically constructed p-$Cu_2O$/n-ZnO heterojunction diode for photovoltaic device, J. Phys. D: Appl. Phys. 40 (2007) 3326–3329.
[58] S. Chu, X. Zheng, F. Kong, G. Wu, L. Luo, Y. Guo, H. Liu, Y. Wang, Architecture of $Cu_2O$@$TiO_2$ core–shell heterojunction and photodegradation for 4-nitrophenol under simulated sunlight irradiation, Mater. Chem. Phys. 129 (3) (2011) 1184–1188.
[59] S. Kakuta, T. Abe, A novel example of molecular hydrogen generation from formic acid at visible-light-responsive photocatalyst, ACS Appl. Mater. Interfaces 1 (2009) 2707–2710.
[60] L. Huang, F. Peng, H. Yu, H. Wang, Preparation of cuprous oxides with different sizes and their behaviors of adsorption, visible-light driven photocatalysis and photocorrosion, Solid. State Sci. 11 (2009) 129–138.
[61] J.E. Turner, M. Hendewerk, J. Parmeter, D. Neiman, G.A. Somorjai, Characterization of doped iron oxide electrodes for the photodissociation of water, J. Electrochem. Soc. 131 (1984) 1777–1783.
[62] H.E. Prakasam, O.M. Varghese, M. Paulose, G.K. Mor, C.A. Grimes, Synthesis and photoelectrochemical properties of nanoporous iron (III) oxide by potentiostatic anodization, Nanotechnology 17 (2006) 4285–4291.
[63] P. Hiralal, S. Saremi-Yarahmadi, B.C. Bayer, H. Wang, S. Hofmann, K.G.U. Wijayantha, G.A.J. Amaratunga, Nanostructured hematite photoelectrochemical electrodes prepared by the low temperature thermal oxidation of iron, Sol. Energy Mater. Sol. Cells 95 (2011) 1819–1825.
[64] R.L. Spray, K.-S. Choi, Photoactivity of transparent nanocrystalline $Fe_2O_3$ electrodes prepared via anodic electrodeposition, Chem. Mater. 21 (2009) 3701–3709.
[65] M. Metikos-Hukovic, The photoelectrochemical properties of anodic $Bi_2O_3$ films, Electrochim. Acta 26 (1981) 989–1000.
[66] G. Li, H.Y. Yip, Ch Hu, P.K. Wong, Preparation of grape-like $Bi_2O_3$/Ti photoanode and its visible light activity, Mater. Res. Bull. 46 (2) (2011) 153–157.
[67] X. Zhao, H. Liu, J. Qu, Photoelectrocatalytic degradation of organic contaminants at $Bi_2O_3$/$TiO_2$ nanotube array electrode, Appl. Surf. Sci. 257 (2001) 4621–4624.
[68] N. Myung, S. Ham, S. Choi, Y. Chae, W.-G. Kim, Y.J. Jeon, K.-J. Paeng, W. Chanmanee, N.R. De Tacconi, K. Rajeshwar, Tailoring interfaces for electrochemical synthesis of semiconductor films: $BiVO_4$, $Bi_2O_3$, or composites, J. Phys. Chem. C 115 (2011) 7793–7800.
[69] S.-Y. Park, B.-W. Cho, K.-S. Yun, Photoelectrochemical properties of bismuth-doped titanium oxide electrodes, J. Appl. Electrochem. 24 (1994) 1133–1138.
[70] M. Miyauchi, A. Nakajima, A. Fujishima, K. Hashimoto, T. Watanabe, Photoinduced surface reaction on $TiO_2$ and $SrTiO_3$ films: Photocatalytic oxidation and photoinduced hydrophilicity, Chem. Mater. 12 (2000) 3–5.
[71] J. Zhang, J.H. Bang, C. Tang, P.V. Kamat, Tailored $TiO_2$-$SrTiO_3$ heterostructure nanotube arrays for improved photoelectrochemical performance, ACS Nano 4 (1) (2010) 387–395.
[72] I.E. Palauskas, J.E. Katz, G.E. Jellison Jr., N.S. Lewis, L.A. Boatner, Photoelectrochemical studies of semiconducting photoanodes for hydrogen production via water dissociation, Thin Solid Films 516 (2008) 8175–8178.
[73] M. Long, W. Cai, J. Cai, B. Zhou, X. Chai, Y. Wu, Efficient photocatalytic degradation of phenol over $Co_3O_4$/$BiVO_4$ composite under visible light irradiation, J. Phys. Chem. B 110 (2006) 20211–20216.
[74] P. Chatchai, S. Kishioka, Y. Murakami, A.Y. Nosaka, Y. Nosaka, Enhanced photoelectrocatalytic activity of FTO/$WO_3$/$BiVO_4$ electrode modified with gold nanoparticles for water oxidation under visible light irradiation, Electrochim. Acta 55 (2010) 592–596.
[75] H.H. Kung, H.S. Jarrett, A.W. Sleight, A. Ferretti, Semiconducting oxide anodes in photoassisted electrolysis of water, J. Appl. Phys. 48 (6) (1977) 2463–2469.
[76] P. Lianos, Production of electricity and hydrogen by photocatalytic degradation of organic wastes in a photoelectrochemical cell. The concept of the Photofuelcell: a review of a re-emerging research field, J. Hazard. Mater. 185 (2011) 575–590.
[77] Y. Takahashi, Y. Matsuoka, Dip-coating of $TiO_2$ films using a sol derived from Ti(O-i-Pr)$_4$-diethanolamine-$H_2O$-i-PrOH system, J. Mater. Sci. 23 (1998) 2259–2266.
[78] B. O'Regan, J. Moser, M. Anderson, M. Gratzel, Vectorial electron injection into transparent semiconductor membranes and electric field effects on the dynamics of light-induced charge separation, J. Phys. Chem. 94 (1990) 8720–8726.
[79] K. Kato, A. Tsuzuki, Y. Torii, H. Taoda, T. Kato, Y. Butsugan, Morphology of thin anatase coatings prepared from alkoxide solutions containing organic polymer, affecting the photocatalytic decomposition of aqueous acetic acid, J. Mater. Sci. 30 (1995) 837–841.
[80] T. Sugimoto, X. Zhou, A. Muramatsu, Synthesis of uniform anatase $TiO_2$ nanoparticles by gel-sol method: 3. Formation process and size control, J. Colloid Interface Sci. 259 (2003) 43–52.
[81] H. Zhang, J.F. Banfield, Size dependence of the kinetic rate constant for phase transformation in $TiO_2$ nanoparticles, Chem. Mater. 17 (2005) 3421–3425.
[82] M.A. Anderson, M.J. Gieselmann, Q. Xu, Titania and alumina ceramic membranes, J. Membr. Sci. 39 (3) (1988) 243–258.
[83] E.A. Barringer, H.K. Bowen, High-purity, monodisperse $TiO_2$ powders by hydrolysis of titanium tetraethoxide. 1. Synthesis and physical properties, Langmuir 1 (1985) 420–428.
[84] J.L. Look, C.F. Zukoski, Colloidal stability and titania precipitate morphology: influenc of short-range repulsions, J.Am. Ceram. Soc. 78 (1995) 21–32.

[85] D. Vorkapic, T. Matsoukas, Reversible agglomeration: a kinetic model for the peptization of titania nanocolloids, J. Colloid Interface Sci. 214 (1999) 283–291.
[86] H. Shin, J. Collins, M.R. De Gurie, A.H. Heuer, C.M. Sukenik, Synthesis and characterization of $TiO_2$ thin films on organic self-assembled monolayers: part I. Film formation from aqueous solutions, J. Mater. Res. 10 (1995) 692–698.
[87] M. Langlet, A. Kim, M. Audier, C. Guillard, J.M. Herrmann, Liquid phase processing and thin film deposition of titania nanocrystallites for photocatalytic applications on thermally sensitive substrates, J. Mater. Sci. 38 (2003) 3945–3953.
[88] M. Anderson, L. Osterlund, S. Ljungstroem, A. Palmqvist, Preparation of nanosize anatase and rutile $TiO_2$ by hydrothermal treatment of microemulsions and their activity for photocatalytic wet oxidation of phenol, J. Phys. Chem.B 106 (2002) 10674–10679.
[89] J. Yang, S. Mei, J.M.F. Ferreira, In situ preparation of weakly flocculated aqueous anatase suspensions by a hydrothermal technique, J. Colloid Interface Sci. 260 (2003) 82–88.
[90] Y. Han, T. Qiu, T. Song, Preparation of ultrafine tungsten powder by sol–gel method, J. Mater. Sci. Technol. 24 (5) (2008) 816–818.
[91] S.-N. Bai, S.-C. Wu, Synthesis of ZnO nanowires by the hydrothermal method, using sol–gel prepared ZnO seed films, J. Mater. Sci.: Mater. Electron. 22 (2011) 339–344.
[92] R. Marczak, F. Werner, R. Ahmad, V. Lobaz, D.M. Guldi, W. Peukert, Detailed investigations of ZnO photoelectrodes preparation for dye sensitized solar cells, Langmuir 27 (2011) 3920.
[93] J. Cao, T. Kako, N. Kikugawa, J. Ye, Photoanodic properties of pulsed-laser-deposited $\alpha$-$Fe_2O_3$ electrode, J. Phys. D: Appl. Phys. 43 (2010) 325101.
[94] A. Watanabe, H. Kozuka, Photoanodic properties of sol–gel-derived $Fe_2O_3$ thin films containing dispersed gold and silver particles, J. Phys. Chem. B 107 (2003) 12713–12720.
[95] L.S. Zhong, J.S. Hu, H.P. Liang, A.M. Cao, W.G. Song, L. Wang, Self-assembled 3D flowerlike iron oxide nanostructures and their application in water treatment, Adv. Mater. 18 (2006) 2426–2431.
[96] R. Subasri, T. Shinohara, Investigations on $SnO_2$–$TiO_2$ composite photoelectrodes for corrosion protection, Electrochem. Commun. 5 (2003) 897–902.
[97] S. Chai, G. Zhao, P. Li, Y. Lei, Y.-N. Zhang, D. Li, Novel sieve-like $SnO_2/TiO_2$ nanotubes with integrated photoelectrocatalysis: fabrication and application for efficient toxicity elimination of nitrophenol wastewater, J. Phys. Chem. 115 (37) (2011) 18261–18269.
[98] P. Chatchai, Y. Murakami, S.-Y. Kishioka, A.Y. Nosaka, Y. Nosaka, $FTO/SnO_2/BiVO_4$ composite photoelectrode for water oxidation under visible light irradiation, Electrochem. Solid State Lett. 11 (6) (2008) H160–H163.
[99] M.M. Patil, V.V. Deshpande, S.R. Dhage, V. Ravi, Synthesis of bismuth oxide nanoparticles at 100 °C, Mater. Lett. 59 (2005) 2523–2525.
[100] X. Zhao, H. Liu, J. Qu, Photoelectrocatalytic degradation of organic contaminants at $Bi_2O_3/TiO_2$ nanotube array electrode, Appl. Surf. Sci. 257 (2011) 4621–4624.
[101] Y.-E. Gu, Y. Zhang, F. Zhang, J. Wei, C. Wang, Y. Du, W. Ye, Investigation of photoelectrocatalytic activity of $Cu_2O$ nanoparticles for p-nitrophenol using rotating ring-disk electrode and application for electrocatalytic determination, Electrochim. Acta 56 (2010) 953–958.
[102] N.J. Peill, M.R. Hoffmann, Development and optimization of a $TiO_2$-coated fiber-optic cable reactor: photocatalytic degradation of 4-chlorophenol, Environ. Sci. Technol. 29 (1995) 2974–2981.
[103] J.A. Byrne, B.R. Eggins, N.M.D. Brown, B. McKinney, Immobilisation of $TiO_2$ powder for the treatment of polluted water, Appl. Catal. B 17 (1998) 25–36.
[104] J. Krysa, J. Jirkovsky, Electrochemically assisted photocatalytic degradation of oxalic acid on particulate $TiO_2$ film in a batch mode plate photoreactor, J. Appl. Electrochem. 32 (2002) 591–596.
[105] Q. Shen, T. Toyoda, Studies of optical absorption and electron transport in nanocrystalline $TiO_2$ electrodes, Thin Solid Films 438 (2003) 167–170.
[106] Q. Shen, D. Arae, T. Toyoda, Photosensitization of nanostructured $TiO_2$ with CdSe quantum dots: effects of microstructure and electron transport in $TiO_2$ substrates, J. Photochem. Photobiol. A 164 (2004) 75–80.
[107] J.A. Glasscock, N. Savvides, Enhancement of photoelectrochemical hydrogen production from hematite thin films by the introduction of Ti and Si, J. Phys.Chem. B 111 (2007) 16477–16488.
[108] A.S. Reddy, S. Uthanna, P.S. Reddy, Properties of dc magnetron sputtered $Cu_2O$ films prepared at different sputtering pressures, Appl. Surf. Sci. 253 (2007) 5287–5292.
[109] L. Kavan, M. Gratzel, Highly efficient semiconducting $TiO_2$ photoelectrodes prepared by aerosol pyrolysis, Electrochim. Acta 40 (1995) 643–652.
[110] A.I. Martinez, D.R. Acosta, A.A. Lopez, Effect of deposition methods on the properties of photocatalytic $TiO_2$ thin films prepared by spray pyrolysis and magnetron sputtering, J. Phys. Condens. Matter 16 (2004) S2335–S2344.
[111] H. Yanagi, Y. Ohoka, T. Hishiki, K. Ajito, A. Fujishima, Characterization of dye-doped $TiO_2$ films prepared by spray-pyrolysis, Appl. Surf. Sci. 113–114 (1997) 426–431.
[112] P.S. Shinde, S.B. Sadale, P.S. Patil, P.N. Bhosale, A. Brüger, M. Neumann-Spallart, Ch. Bhosale, Properties of spray deposited titanium dioxide thin films and their application in photoelectrocatalysis, Sol. Energy Mater. Sol. Cells 92 (3) (2008) 283–290.
[113] A. Enesca, A. Duta, M. Nanu, C. Enache, R. Van der Krol, J. Schoonman, Photoelectrode materials of tungsten oxide ($WO_3$) for water splitting, in: Proceedings of the International Semiconductor Conference, vol. 2, 2005, pp. 293–296.
[114] R. Sivakumar, A.M.E. Raj, B. Subramanian, M. Jayachandran, D.C. Trivedi, C. Sanjeeviraja, Preparation and characterization of spray deposited n-type $WO_3$ thin films for electrochromic devices, Mater. Res. Bull. 39 (10) (2004) 1479–1489.
[115] M. Regragui, M. Addou, A. Outzourhit, E. El Idrissi, A. Kachouane, A. Bougrine, Electrochromic effect in $WO_3$ thin films prepared by spray pyrolysis, Sol. Energy Mater. Sol. Cells 77 (4) (2003) 341–350.
[116] P.S. Patil, P.R. Patil, Studies on the photoelectrochemical cell formed with $WO_3$ photoanode by using Gartner's model, Bull. Mater. Sci. 19 (4) (1996) 651–656.
[117] S.U.M. Khan, J.J. Akikusa, Photoelectrochemical splitting of water at nanocrystalline n-$Fe_2O_3$ thin-film electrodes, Phys. Chem. B 103 (1999) 7184–7189.
[118] C.J. Sartoretti, B.D. Alexandr, R. Solarska, I.A. Rutkowska, J. Augustynski, R. Cerny, Photoelectrochemical oxidation of water at transparent ferric oxide film electro, J. Phys. Chem. B 109 (2005) 13685–13692.
[119] R. Ayouchi, F. Martin, D. Leinen, J.R. Ramos-Barrado, Growth of pure ZnO thin films prepared by chemical spray pyrolysis on silicon, J. Cryst. Growth 247 (2003) 497–504.
[120] D. Davazoglou, A. Donnadieu, O. Bohnke, Electrochromic effect in $WO_3$ thin films prepared by CVD, Sol. Energy Mater. Sol. Cells 16 (1-3) (1987) 55–65.
[121] D. Gogova, A. Iossifova, T. Ivanova, Zl. Dimitrova, K. Gesheva, Electrochromic behavior in CVD grown tungsten oxide films, J. Cryst.Growth 198–199 (1999) 1230–1234.
[122] M. Hitchman, F. Tian, Studies of $TiO_2$ thin films prepared by chemical vapour deposition for photocatalytic and photoelectrocatalytic degradation of 4-chlorophenol, J. Electroanal. Chem. 538–539 (2002) 165–172.
[123] T.N. Murakami, Y. Kijitori, N. Kawashima, T. Miyasaka, Low temperature preparation of mesoporous $TiO_2$ films for efficient dye-sensitized photoelectrode by chemical vapor deposition combined with UV light irradiation, J. Photochem. Photobiol. A 164 (1–3) (2004) 187–191.
[124] T. Ivanova, K.A. Gesheva, M. Kalitzova, B. Marsen, B. Cole, E.L. Miller, Electrochromic behavior of Mo/W oxides related to their surface morphology and intercalation process parameters, Mater. Sci. Eng. B 142 (2-3) (2007) 126–134.
[125] G. Li Puma, A. Bono, D. Krishnaiah, J.G. Collin, Preparation of titanium dioxide photocatalyst loaded onto activated carbon support using chemical vapor deposition: a review paper, J. Hazard. Mater. 157 (2-3) (2008) 209–219.
[126] T. Ivanova, K.A. Gesheva, M. Kalitzova, F. Hamelmann, F. Luekermann, U. Heinzmann, Electrochromic mixed films based on $WO_3$ and $MoO_3$, obtained by an APCVD method, J. Optoelectron. Adv. Mater. 11 (10) (2009) 1513–1516.
[127] U. Bjorksten, J. Moser, M. Gratzel, Photoelectrochemical studies on nanocrystalline hematite films, Chem. Mater. 6 (1994) 858–863.
[128] A. Duret, M. Gratzel, Visible light-induced water oxidation on mesoscopic $\alpha$-$Fe_2O_3$ films made by ultrasonic spray pyrolysis, J. Phys. Chem. B 109 (2005) 17184–17191.
[129] A. Hongsingthong, I.A. Yunaz, S. Miyajima, M. Konagai, Preparation of ZnO thin films using MOCVD technique with $D_2O/H_2O$ gas mixture for use as TCO in silicon-based thin film solar cells, Sol. Energy Mater. Sol. Cells 95 (2011) 171–174.
[130] L. Hechavarria, H. Hu, M. Miranda, M.E. Nicho, Electrochromic responses of low-temperature-annealed tungsten oxide thin films in contact with a liquid and a polymeric gel electrolyte, J. Solid State Electrochem. 13 (5) (2009) 687–695.
[131] I. Saeki, N. Okushi, H. Konno, R. Furuichi, The photoelectrochemical response of $TiO_2$–$WO_3$ mixed oxide films prepared by thermal oxidation of titanium coated with tungsten, J. Electrochem. Soc. 143 (7) (1996) 2226–2230.
[132] D. Velten, V. Biehl, F. Aubertin, B. Valeske, W. Possart, J. Breme, Preparation of $TiO_2$ layers on cp-Ti and Ti6Al4V by thermal and anodic oxidation and by sol–gel coating techniques and their characterization, J. Biomed. Mater. Res. 59 (1) (2002) 18–28.
[133] S.-Y. Park, B.-W. Cho, K.-S. Yun, E.-C. Lee, Photoelectrochemical properties of bismuth-doped titanium oxide electrodes, J. Appl. Electrochem. 24 (1994) 1133–1138.
[134] R. Shinar, J.H. Kennedy, Photoactivity of doped $\alpha$-$Fe_2O_3$ electrodes, Sol. Energy Mater. 6 (1982) 323–335.
[135] C. Natarajan, G. Nogami, Cathodic electrodeposition of nanocrystalline titanium dioxide thin films, J. Electrochem. Soc. 143 (1996) 1547–1550.
[136] I. Zhitomirsky, L. Gal-Or, A. Khon, H.W. Hennicke, Electrodeposition of ceramic films from non-aqueous and mixed solutions, J. Mater. Sci. 30 (1995) 5307–5312.
[137] C.R. Chenthamarakshan, N.R. De Tacconi, K. Rajeshwar, R. Shiratsuchi, Immobilizing semiconductor particles by occlusion electrosynthesis in an oxide film matrix: the titania model case, Electrochem. Commun. 4 (2002) 871–876.
[138] J. Yamamoto, A. Tan, R. Shiratsuchi, S. Hayase, C.R. Chenthamarakshan, K. Rajeshwar, A 4% efficient dye-sensitized solar cell fabricated from cathodically electrosynthesized composite titania films, Adv. Mater. 15 (21) (2003) 1823–1825.
[139] S. Karuppuchamy, D.P. Amalnerkar, K. Yamaguchi, T. Yoshida, T. Sugiura, H. Minoura, Cathodic electrodeposition of $TiO_2$ thin films for dye-sensitized photoelectrochemical applications, Chem. Lett. 143 (2001) 78–79.
[140] S. Karuppuchamy, K. Nonomura, T. Yoshida, T. Sugiura, H. Minoura, Cathodic electrodeposition of oxide semiconductor thin films and their application to dye-sensitized solar cells, Solid State Ionics 151 (2002) 19–27.
[141] I. Zhitomirsky, L. Gal-Or, Cathodic electrosynthesis of ceramic deposits, J. Eur. Ceram. Soc. 16 (1996) 819–824.

[142] I. Zhitomirsky, Cathodic electrosynthesis of titania films and powders, Nanostruct. Mater. 8 (1997) 521–528.
[143] I. Zhitomirsky, L. Gal-Or, A. Khon, M.D. Spang, Electrolytic PZT films, J. Mater. Sci. 32 (1997) 803–807.
[144] I. Zhitomirsky, Cathodic electrosynthesis of titanium and ruthenium oxides, Mater. Lett. 33 (1998) 305–310.
[145] I. Zhitomirsky, Electrolytic deposition of oxide films in the presence of hydrogen peroxide, J. Eur. Ceram. Soc. 19 (1999) 2581–2587.
[146] K. Kamada, M. Mukai, Y. Matsumoto, Electrodeposition of titanium(IV) oxide film from sacrificial titanium anode in $I_2$-added acetone bath, Electrochim. Acta 47 (2002) 3309–3313.
[147] Y. Matsumoto, Y. Ishikawa, M. Nichida, S. Li, A new electrochemical method to prepare mesoporous titanium(IV) oxide photocatalyst fixed on alumite substrate, J. Phys. Chem. B 104 (2000) 4204–4209.
[148] Y. Ishikawa, Y. Matsumoto, Electrodeposition of $TiO_2$ photocatalyst into nanopores of hard alumite, Electrochim. Acta 46 (2001) 2819–2824.
[149] Y. Ishikawa, Y. Hayashi, Y. Matsumoto, Preparation of titanium(IV) oxide film on a hard alumite substrate, J. Mater. Res. 17 (2002) 2373–2378.
[150] Y. Ishikawa, Y. Matsumoto, Preparation of titanium (IV) oxide film on a hard alumite substrate, Solid State Ionics 151 (2002) 213–218.
[151] M. Zhou, N.R. De Tacconi, K. Rajeshwar, Preparation and characterization of nanocrystalline composite (nanocomposite) films of titanium dioxide and nickel by occlusion electrodeposition, J. Electroanal. Chem. 421 (1997) 111–120.
[152] N.R. De Tacconi, H. Wenren, D. McChesney, K. Rajeshwar, Photoelectrochemical oxidation of formate ions on nickel-titanium dioxide nanocomposite electrodes: unusually high current doubling yields and manifestation of a site proximity effect, Langmuir 14 (1998) 2933–2935.
[153] N.R. De Tacconi, C.A. Boyles, K. Rajeshwar, Surface morphology/composition and photoelectrochemical behavior of metal–semiconductor composite films, Langmuir 16 (3) (2000) 5665–5672.
[154] S. Somasundaram, C.R. Chenthamarakshan, K. Rajeshwar, N.R. Tacconi, Photoelectrochemical behavior of composite metal oxide semiconductor films with a $WO_3$ matrix and occluded Degussa P 25 $TiO_2$ particles, J. Electroanal. Chem. 577 (2005) 167–177.
[155] D. Matthews, A. Kay, M. Gratzel, Electrophoretically deposited titanium dioxide thin films for photovoltaic cells, Aust. J. Chem. 47 (1994) 1869–1877.
[156] S. Peulon, D. Lincot, Cathodic electrodeposition from aqueous solution of dense or open-structured zinc oxide films, Adv. Mater. 8 (1996) 166–170.
[157] S. Peulon, D. Lincot, Mechanistic study of cathodic electrodeposition of zinc oxide and zinc hydroxychloride films from oxygenated aqueous zinc chloride solutions, J. Electrochem. Soc. 145 (1998) 864.
[158] J. Katayama, K. Ito, M. Matsouka, J. Tamaki, Performance of $Cu_2O$/ZnO solar cell prepared by two-step electrodeposition, J. Appl. Electrochem. 34 (2004) 687–692.
[159] S.-I. Na, S.-S. Kim, W.-K. Hong, J.-W. Park, J. Jo, Y.-C. Nah, T. Lee, D.-Y. Kim, Fabrication of $TiO_2$ nanotubes by using electrodeposited ZnO nanorod template and their application to hybrid solar cells, Electrochim. Acta 53 (2008) 2560–2566.
[160] J. Cui, U.J. Gibson, A simple two-step electrodeposition of $Cu_2O$/ZnO Nanopillar solar cells, J. Phys. Chem C 114 (2010) 6408–6412.
[161] P. Atienzar, T. Ishwara, B.N. Illy, M.P. Ryan, B.C. O'Regan, J.R. Durrant, J. Nelson, Control of photocurrent generation in polymer/ZnO nanorod solar cells by using a solution-processed $TiO_2$ overlayer, J. Phys. Chem. Lett. 1 (2010) 708–713.
[162] J. Chen, H. Ye, L. Ae, Y. Tang, D. Kieven, Th Rissom, J. Neuendorf, M.Ch. Lux-Steiner, Tapered aluminum-doped vertical zinc oxide nanorod arrays as light coupling layer for solar energy applications, Sol. Energy Mater. Sol. Cells 95 (2011) 1437–1440.
[163] R. Schrebler, K. Bello, F. Vera, P. Cury, E. Munoz, R. Del Rio, H. Gomez Meier, R. Gordova, E.A. Dalchiele, An electrochemical deposition route for obtaining $\alpha$-Fe $_2O_3$ thin films, Electrochem. Solid-State Lett. 9 (2006) C110–C113.
[164] R. Schrebler, C. Llewelyn, F. Vera, P. Cury, E. Munoz, R. Del Rio, H. Gomez Meier, R. Gordova, E.A. Dalchiele, An electrochemical deposition route for obtaining $\alpha$-Fe $_2O_3$ thin films: II. EQCM study and semiconductor properties, Electrochem. Solid-State Lett. 10 (2007) D95–D99.
[165] T. Pauporte, A simplified method for $WO_3$ electrodeposition, J. Electrochem. Soc. 149 (11) (2002) C539–C545.
[166] T. Pauporte, A. Goux, A. Kahn-Harari, N.R. De Tacconi, C.R. Chenthamarakshan, K. Rajeshwar, D. Lincot, Cathodic electrodeposition of mixed oxide thin films, J. Phys. Chem. Solids 64 (2003) 1737–1742.
[167] N.R. De Tacconi, C.R. Chenthamarakshan, K. Rajeshwar, T. Pauporte, D. Lincot, Pulsed electrodeposition of $WO_3$-$TiO_2$ composite films, Electrochem. Commun. 5 (2003) 220–224.
[168] J. Georgieva, S. Armyanov, E. Valova, Ts Tsacheva, I. Poulios, S. Sotiropoulos, Photoelectrochemical behaviour of electrodeposited tungsten trioxide and electrosynthesised titanium dioxide single component and bilayer coatings on stainless steel substrates, J. Electroanal. Chem. 585 (2005) 35–43.
[169] J. Georgieva, S. Armyanov, E. Valova, I. Poulios, S. Sotiropoulos, Enhanced photocatalytic activity of electrosynthesised tungsten trioxide-titanium dioxide bi-layer coatings under ultraviolet and visible light illumination, Electrochem. Commun. 9 (2007) 365–370.
[170] J. Georgieva, S. Armyanov, E. Valova, N. Phillipides, I. Poulios, S. Sotiropoulos, Photoelectrocatalytic activity of electrosynthesised tungsten trioxide–titanium dioxide bi-layer coatings for the photooxidation of organics, J. Adv. Oxid.Technol. 11 (2008) 300–307.
[171] T.D. Golden, M.G. Shumsky, Y. Zhou, R.A. Van der Werf, R.A. Van Leeuwen, J.A. Switzer, Electrochemical deposition of copper(I) oxide films, Chem. Mater. 8 (1996) 2499–2504.
[172] Y. Zhou, J.A. Switzer, Electrochemical deposition and microstructure of copper (I) oxide films, Scripta Mater. 38 (1998) 1731–1738.
[173] W. Septina, S. Ikeda, M. Alam Khan, T. Hirai, T. Harada, M. Matsumura, L.M. Peter, Potentiostatic electrodeposition of cuprous oxide thin films for photovoltaic applications, Electrochim. Acta 56 (2011) 4882–4888.
[174] E. Smotkin, A.J. Bard, A. Campion, M.A. Fox, T. Malllouk, S.E. Webber, J.M. White, Bipolar $TiO_2$/Pt semiconductor photoelectrodes and multielectrode arrays for unassisted photolytic water splitting, J. Phys. Chem. 90 (19) (1986) 4604–4607.
[175] X.Z. Li, H.L. Liu, F.B. Li, C.L. Mak, Photoelectrocatalytic oxidation of rhodamine B in aqueous solution using Ti/$TiO_2$ mesh photoelectrodes, J. Environ. Sci. Health Part A Environ. Sci. Health Part A Environ. Sci. Eng. 37 (1) (2002) 55–69.
[176] K.S. Raja, M. Misra, V.K. Mahajan, T. Gandhi, P. Pillai, S.K. Mohapatra, Photo-electrochemical hydrogen generation using band-gap modified nanotubular titanium oxide in solar light, J. Power Sources 161 (2) (2006) 1450–1457.
[177] Y. Xie, Photoelectrochemical application of nanotubular titania photoanode, Electrochim. Acta 51 (17) (2006) 3399–3406.
[178] C.J. Lin, Y.T. Lu, C.H. Hsieh, S.H. Chien, Surface modification of highly ordered $TiO_2$ nanotube arrays for efficient photoelectrocatalytic water splitting, Appl. Phys. Lett. 94 (11) (2009) (Article no.113102).
[179] A.Z. Sadek, H. Zheng, K. Latham, W. Wlodarski, K. Kalantar-Zadeh, Anodization of Ti thin film deposited on ITO, Langmuir 25 (1) (2009) 509–514.
[180] K.L. Hardee, A.J. Bard, Semiconductor electrodes. X. Photoelectrochemical behavior of several polycrystalline metal oxide electrodes in aqueous solutions, J. Electrochem. Soc. 124 (2) (1977) 215–224.
[181] B. Reichman, A.J. Bard, Semiconductor electrodes. 22. Electrochromism and photoelectrochemistry at $WO_3$ layers prepared by thermal and anodic oxidation of W, J. Electrochem. Soc. 126 (12) (1979) 2133–2139.
[182] N.R. De Tacconi, C.R. Chenthamarakshan, G. Yogeeswaran, A. Watchharenwong, R.S. De Zoysa, N.A. Basit, K. Rajeswar, Nanoporous $TiO_2$ and WO3 films by anodization of titanium and tungsten substrates: Influence of process variables on morphology and photoelectrochemical response, J. Phys. Chem. B 110 (50) (2006) 25355–25374.
[183] A. Watcharenwong, W. Chanmanee, N.R. De Tacconi, C.R. Chenthamarakshan, P. Kajitvichyanukul, K. Rajeshwar, Anodic growth of nanoporous $WO_3$ films: morphology, photoelectrochemical response and photocatalytic activity for methylene blue and hexavalent chrome conversion, J. Electroanal. Chem. 612 (1) (2008) 112–120.
[184] E. Fortin, D. Masson, Photovoltaic effects in $Cu_2O$/Cu solar cells grown by anodic oxidation, Solid-State Electron. 25 (1982) 281–283.
[185] L. Kavan, B. O'Regan, A. Kay, M. Grätzel, Preparation of $TiO_2$ (anatase) films on electrodes by anodic oxidative hydrolysis of $TiCl_3$, J. Electroanal. Chem. 346 (1993) 291–307.
[186] S. Somasundaram, C.R. Chenthamarakshan, N.R. De Tacconi, N.A. Basit, K. Rajeshwar, Composite $WO_3$–$TiO_2$ films: pulsed electrodeposition from a mixed bath versus sequential deposition from twin baths, Electrochem. Commun. 8 (2006) 539–543.
[187] D. Jiang, H. Zhao, Z. Jia, J. Cao, R. John, Photoelectrochemical behaviour of methanol oxidation at nanoporous $TiO_2$ film electrodes, J. Photochem. Photobiol. A 144 (2001) 197–204.
[188] G. Waldner, M. Pourmodjib, R. Bauer, M. Neumann-Spallart, Chemosphere 50 (2003) 989–998.
[189] Y. Hou, J. Qu, X. Zhao, P. Lei, D. Wan, C.P. Huang, Electro-photocatalytic degradation of acid orange II using a novel $TiO_2$/ACF photoanode, Sci. Total Environ. 407 (7) (2009) 2431–2439.
[190] B. Gao, C. Peng, G.Z. Chen, G. Li Puma, Photo-electro-catalysis enhancement on carbon nanotubes/titanium dioxide (CNTs/$TiO_2$) composite prepared by a novel surfactant wrapping sol–gel method, Appl. Catal. 85 (1–2) (2008) 17–23.
[191] F.J. Zhang, M.L. Chen, W.C. Oh, Photocatalytic degradation of methylene blue by CNT/$TiO_2$ composites prepared from MWCNT and titanium n-butoxide with benzene, Korean J. Mater. Res. 18 (11) (2008) 583–591.
[192] J. Qu, X. Zhao, Design of BDD–$TiO_2$ hybrid electrode with P–N function for photoelectroatalytic degradation of organic contaminants, Environ. Sci. Technol. 42 (13) (2008) 4934–4939.
[193] A. Manivannan, N. Spataru, K. Arihara, A. Fujishima, Electrochemical deposition of titanium oxide on boron-doped diamond electrodes, Electrochem. Solid-State Lett. 8 (10) (2005) C138–C140.
[194] J. Shang, W. Li, Y. Zhu, Structure and photocatalytic characteristics of $TiO_2$ film photocatalyst coated on stainless steel webnet, J. Mol. Catal. A: Chem. 202 (2003) 187–195.
[195] A.H.C. Chan, C.K. Chan, J.P. Barford, J.F. Porter, Solar photocatalytic thin film cascade reactor for treatment of benzoic acid containing wastewater, Water Res. 37 (5) (2003) 1125–1135.
[196] J.H. Park, Y. Jun, H.G. Yun, S.Y. Lee, M.G. Kang, Fabrication of an efficient dye-sensitized solar cell with stainless steel substrate, J. Electrochem. Soc. 155 (7) (2008) F145–F149.
[197] M.A. Greenwood, Solar cells of stainless steel, Photon. Spectra 42 (5) (2008) 94–95.

[198] K. Miettunen, J. Halme, M. Toivola, P. Lund, Initial performance of dye solar cells on stainless steel substrates, J. Phys. Chem. C 112 (10) (2008) 4011–4017.
[199] K. Vinodgopal, P.V. Kamat, Enhanced rates of photocatalytic degradation of an azo dye using $SnO_2/TiO_2$ coupled semiconductor thin films, Environ. Sci. Technol. 29 (1995) 841–845.
[200] C.H. Wu, C.L. Chang, Decolorization of Reactive Red 2 by advanced oxidation processes: comparative studies of homogeneous and heterogeneous systems, J. Hazard. Mater. 128 (2006) 265–272.
[201] F.U. Xianzhi, L.A. Clark, Q. Yang, M.A. Anderson, Enhanced photocatalytic performance of titania-based binary metal oxides: $TiO_2/SiO_2$ and $TiO_2/ZrO_2$, Environ. Sci. Technol. 30 (1996) 647–653.
[202] Y. Hu, H.L. Tsai, C.L. Huang, Effect of brookite phase on the anatase-rutile transition in titania nanoparticles, J. Eur. Ceram. Soc. 23 (2003) 691–696.
[203] J. Papp, S. Soled, K. Dwight, A. Wold, Surface acidity and photocatalytic activity of $TiO_2$, $WO_3/TiO_2$, and $MoO_3/TiO_2$ photocatalysts, Chem. Mater. 6 (1994) 496–500.
[204] A.G. Agrios, P. Pichat, State of the art and perspectives on materials and applications of photocatalysis over $TiO_2$, J. Appl. Electrochem. 35 (2005) 655–663.
[205] B. O'Regan, M. Gratzel, A low-cost, high-efficiency solar cell based on dye-sensitized colloidal $TiO_2$ films, Nature (London) 353 (1991) 737–740.
[206] N. Lu, H. Zhao, J. Li, X. Quan, S. Chen, Characterization of boron-doped $TiO_2$ nanotube arrays prepared by electrochemical method and its visible light activity, Sep. Purif. Technol. 62 (3) (2008) 668–673.
[207] Y. Su, S. Han, X. Zhang, X. Chen, L. Lei, Preparation and visible-light-driven photoelectrocatalytic properties of boron-doped $TiO_2$ nanotubes, Mater. Chem. Phys. 110 (2–3) (2008) 239–246.
[208] S.J. Hong, S. Lee, J.S. Jang, Heterojunction $BiVO_4/WO_3$ electrodes for enhanced photoactivity of water oxidation, Energy Environ. Sci. 4 (5) (2011) 1781–1787.
[209] K. Vinodgopal, P.V. Kamat, V. Prashant, Electrochemically assisted photocatalysis using nanocrystalline semiconductor thin films, Sol. Energy Mater. Sol. Cells 38 (1995) 401–410.
[210] Y. Hou, X. Li, X. Zou, X. Quan, G. Chen, Photoeletrocatalytic activity of a $Cu_2O$-loaded self-organized highly oriented $TiO_2$ nanotube array electrode for 4-chlorophenol degradation, Environ. Sci. Technol. 43 (2009) 858–863.
[211] Y. Wang, L. Cai, Y. Li, Y. Tang, Ch Xie, Structural and photoelectrocatalytic characteristic of $ZnO/ZnWO_4/WO_3$ nanocomposites with double heterojunctions, Physica E 43 (2010) 503–509.
[212] G. Xi, B. Yue, J. Cao, J. Ye, $Fe_3O_4/WO_3$ hierarchical core–shell structure: high-performance and recyclable visible-light photocatalysis, Chem. Eur. J. 17 (2011) 5145–5154.
[213] J. Georgieva, S. Armyanov, E. Valova, I. Poulios, S. Sotiropoulos, Preparation and photoelectrochemical characterisation of electrosynthesised titanium dioxide deposits on stainless steel substrates, Electrochim. Acta 51 (10) (2006) 2076–2087.
[214] J. Georgieva, S. Sotiropoulos, S. Armyanov, N. Philippidis, I. Poulios, Photoelectrocatalytic activity of bi-layer $TiO_2/WO_3$ coatings for the degradation of 4-chlorophenol: effect of morphology and catalyst loading, J. Appl. Electrochem. 41 (2011) 173–181.
[215] E. Valova, J. Georgieva, S. Armyanov, S. Sotiropoulos, A.##K. Hubin, Baert M. Raes, Morphology, structure and photoelectrocatalytic activity of $TiO_2/WO_3$ coatings obtained by pulsed electrodeposition onto stainless steel, J. Electrochem. Soc. 157 (2010) D309–D315.
[216] H.O. Finklea, Semiconductor electrodes, in: H.O. Finklea (Ed.), Studies in Physical and Theoretical Chemistry, Elsevier, Amsterdam, 1988, pp. 27–30.
[217] N. Sato, Electrochemistry at Metal and Semiconductor Electrodes, Elsevier, Amsterdam, 1998, pp. 325–371.
[218] Y. Ohko, S. Saitoh, F. Tatsuma, A. Fujishima, Photoelectrochemical anticorrosion and self-cleaning effects of a $TiO_2$ coating for type 304 stainless steel, J. Electrochem. Soc. 148 (1) (2001) B24–B28.
[219] B. O'Regan, J. Moser, V. Gratzel, Vectorial electron injection into transparent semiconductor membranes and electric field effects on the dynamics of light-induced charge separation, J. Phys. Chem. 94 (1990) 8720–8726.
[220] K. Vinodgopal, S. Hotchandani, P.V. Kamat, Electrochemically assisted photocatalysis. $TiO_2$ particulate film electrodes for photocatalytic degradation of 4-chlorophenol, J. Phys. Chem. 97 (1993) 9040–9044.
[221] S. Sodergren, A. Hagfeldt, J. Olsson, S.E. Lindquist, Theoretical models for the action spectrum and the current–voltage characteristics of microporous semiconductor films in photoelectrochemical cells, J. Phys. Chem. 98 (1994) 5552–5556.
[222] W.W. Gartner, Depletion-layer photoeffects in semiconductors, Phys. Rev. 116 (1959) 84–87.
[223] M.A. Butler, Photoelectrolysis and physical properties of the semiconducting electrode $WO_3$, J. Appl. Phys. 48 (1977) 1914–1920.
[224] J. Georgieva, S. Sotiropoulos, S. Armyanov, I. Poulios, Effect of $TiO_2/WO_3/C$ photoanode composition on the photocurrent of all-solid photoelectrochemical cells, Int. J. Nanopart. 4 (2–3) (2011) 216–230.